International Journal for Uncertainty Quantification, 13(4):23–59 (2023)

HIGH-DIMENSIONAL STOCHASTIC DESIGN OPTIMIZATION UNDER DEPENDENT RANDOM VARIABLES BY A DIMENSIONALLY DECOMPOSED GENERALIZED POLYNOMIAL CHAOS EXPANSION

Dongjin Lee & Sharif Rahman*

Department of Mechanical Engineering, The University of Iowa, Iowa City, Iowa 52242, USA

*Address all correspondence to: Dongjin Lee, Department of Mechanical Engineering, The University of Iowa, Iowa City, Iowa 52242, USA, E-mail: dongjin-lee@uiowa.edu

Original Manuscript Submitted: 2/28/2022; Final Draft Received: 1/15/2023

Newly restructured generalized polynomial chaos expansion (GPCE) methods for high-dimensional design optimization in the presence of input random variables with arbitrary, dependent probability distributions are reported. The methods feature a dimensionally decomposed GPCE (DD-GPCE) for statistical moment and reliability analyses associated with a high-dimensional stochastic response; a novel synthesis between the DD-GPCE approximation and score functions for estimating the first-order design sensitivities of the statistical moments and failure probability; and a standard gradient-based optimization algorithm, constructing the single-step DD-GPCE and multipoint single-step DD-GPCE (MPSS-DD-GPCE) methods. In these new design methods, the multivariate orthonormal basis functions are assembled consistent with the chosen degree of interaction between input variables and the polynomial order, thus facilitating to deflate the curse of dimensionality to the extent possible. In addition, when coupled with score functions, the DD-GPCE approximation leads to analytical formulae for calculating the design sensitivities. More importantly, the statistical moments, failure probability, and their design sensitivities are determined concurrently from a single stochastic analysis or simulation. Numerical results affirm that the proposed methods yield accurate and computationally efficient optimal solutions of mathematical problems and design solutions for simple mechanical systems. Finally, the success in conducting stochastic shape optimization of a bogie side frame with 41 random variables demonstrates the power of the MPSS-DD-GPCE method in solving industrial-scale engineering design problems.

KEY WORDS: *RDO, RBDO, statistical moment analysis, reliability analysis, GPCE, dimensionally decomposed GPCE, design sensitivity analysis, score functions, stochastic optimization*

1. INTRODUCTION

Robust design optimization (RDO) and reliability-based design optimization (RBDO), commonly referred to as stochastic design optimization, are the predominant drivers for engineering design when confronted with uncertainties stemming from material properties, manufacturing processes, and operating environments [1–8]. RDO strives to improve the product quality by minimizing the objective function considering the mean and variance of a performance function, leading to an insensitive design. On the other hand, RBDO—another major archetype of stochastic design optimization—aims to achieve high reliability of an optimal design by satisfying the constraints at desired probability levels [9]. The objective function of RDO can be unified with the probabilistic constraints of RBDO, which is regarded as an extension of RBDO or reliability-based robust design optimization. A growing number of studies concerning RDO and RBDO are being published every year with real-world applications, such as those found in the design of aerospace [10,11], automotive [12,13], civil [14], and electronic structures [15] or devices [16].

A stochastic design optimization, whether RDO or RBDO, is grounded on uncertainty quantification (UQ) analysis of complex systems where an output function of interest is often defined algorithmically via finite-element analysis (FEA). In this regard, RDO and RBDO easily become too expensive when UQ is performed via traditional Monte

Carlo simulation (MCS). Therefore, numerous studies on RDO and RBDO have been conducted using multiple surrogate approximations, including polynomial response surface [17], polynomial chaos expansion [18,19], polynomial dimensional decomposition [8], support vector machine [20], artificial neural network [21], and Gaussian process or Kriging [22,23], to name a few. Additionally, the works of Kouri and Shapiro [24], Kolvenbach et al. [25], and Conti et al. [26] in solving stochastic optimization problems constrained by partial differential equations deserve attention. Some of these methods, especially the expansion or decomposition methods, are based on the assumption that the input random variables follow independent probability distributions. However, in reality, there exists significant correlation or dependence among input variables. Indeed, neglecting these correlations or dependencies, whether emanating from loads, material properties, or manufacturing variables, may produce inaccurate or unknowing risky designs [9,27–29]. Having said so, there exist surrogate methods, prominently the Gaussian process models, which can handle independent or dependent probability distributions.

Only a few works introduce polynomial chaos expansion [30–33] or its variants [34,35] for UQ analysis under arbitrary, dependent input variables. More significantly, a generalized polynomial chaos expansion (GPCE) has been successfully employed for the statistical moment and reliability analyses and their design sensitivity analysis, leading to accurate and computationally efficient solutions of RDO and RBDO problems under dependent input random variables; see Refs. [9,29]. There are also other surrogate-based design works [27,36]. However, for truly high-dimensional systems, the RDO and RBDO methods require astronomically large numbers of basis functions, succumbing to the curse of dimensionality. For practical applications, encountering a large number of input variables, say, over 30, is not uncommon. Therefore, developments of new or appropriately modified computational methods, capable of tackling high-dimensional RDO and RBDO problems above and beyond the foregoing works, are desirable.

This paper presents novelly restructured GPCE methods for high-dimensional stochastic design optimization of complex engineering systems under dependent input random variables. The method entails (1) a dimensionally decomposed GPCE (DD-GPCE) for statistical moment and reliability analyses of a high-dimensional stochastic response; (2) a novel fusion of the DD-GPCE approximation and score functions for estimating the first-order design sensitivities of the statistical moments and failure probability; and (3) a standard gradient-based optimization algorithm, constructing single-step DD-GPCE and multipoint single-step DD-GPCE (MPSS-DD-GPCE) methods. Here, the MPSS leverages the single-point method [7] and the multipoint approximation method [37] for obtaining accurate optimal solutions with fewer evaluations of the surrogate.

The paper is organized as follows. Section 2 defines typical RDO and RBDO problems with their concomitant mathematical statements. Section 3 introduces DD-GPCE for statistical moment and reliability analyses, exploiting a three-step algorithm to construct a measure-consistent multivariate orthonormal polynomial basis and standard least-squares regression to estimate the expansion coefficients. Section 4 presents the explicit form of the score function and discloses new analytical sensitivity methods by embedding score functions with the DD-GPCE approximation. Section 5 illustrates the single-step and multipoint single-step design process for solving RDO and RBDO problems and explains how the DD-GPCE-based methods for the statistical moment, failure probability, and their design sensitivity analyses are coupled with a gradient-based optimization algorithm. Section 6 involves three numerical examples, ranging from simple mathematical functions to an industrial-scale engineering problem, conducted to determine the accuracy, convergence properties, and computational efforts of the proposed methods. In the end, Section 7 presents the conclusions of this work.

2. ROBUST AND RELIABILITY-BASED DESIGN OPTIMIZATION

Let $\mathbb{N}$, $\mathbb{N}_0$, $\mathbb{R}$, and $\mathbb{R}_0^+$ be the sets of positive integers, non-negative integers, real numbers, and non-negative real numbers, respectively. For a positive integer $N \in \mathbb{N}$, denote by $\mathbb{R}^N$ the N-dimensional real vector space. Then, denote by $\mathbb{A}^N \subseteq \mathbb{R}^N$ and $\bar{\mathbb{A}}^N \subseteq \mathbb{R}^N$ two bounded or unbounded domains.

Consider a measurable space $(\Omega_{\mathbf{d}}, \mathcal{F}_{\mathbf{d}})$, where $\Omega_{\mathbf{d}}$ is a sample space and $\mathcal{F}_{\mathbf{d}}$ is a σ-field on $\Omega_{\mathbf{d}}$. Defined over $(\Omega_{\mathbf{d}}, \mathcal{F}_{\mathbf{d}})$, let $\{\mathbb{P}_{\mathbf{d}} : \mathcal{F}_{\mathbf{d}} \to [0,1]\}$ be a family of probability measures where, for $M \in \mathbb{N}$ and $N \in \mathbb{N}$, $\mathbf{d} = (d_1, \ldots, d_M)^T \in \mathcal{D}$ is an M-dimensional design vector with nonempty closed set $\mathcal{D} \subset \mathbb{R}^M$. Here, $\mathbf{X} := (X_1, \ldots, X_N)^T : (\Omega_{\mathbf{d}}, \mathcal{F}_{\mathbf{d}}) \to (\mathbb{A}^N, \mathcal{B}^N)$ is an $\mathbb{A}^N$-valued input random vector with $\mathcal{B}^N$ representing the

Borel σ-field on $\mathbb{A}^N$, describing the randomness arising in loads, material properties, and geometry of a complex mechanical system. It is assumed that $\mathbf{X}$ has an absolutely continuous joint distribution function and a continuous joint probability density function (PDF) $f_{\mathbf{X}}(\mathbf{x};\mathbf{d})$ with a bounded or unbounded support $\mathbb{A}^N \subseteq \mathbb{R}^N$. Therefore, the probability law of $\mathbf{X}$ is completely defined by a family of the PDF $\left\{f_{\mathbf{X}}(\mathbf{x};\mathbf{d}) : \mathbf{x} \in \mathbb{R}^N,\ \mathbf{d} \in \mathcal{D}\right\}$ that is associated with probability measures $\{\mathbb{P}_{\mathbf{d}} :\ \mathbf{d} \in \mathcal{D}\}$, so that the probability triple $(\Omega_{\mathbf{d}}, \mathcal{F}_{\mathbf{d}}, \mathbb{P}_{\mathbf{d}})$ of $\mathbf{X}$ depends on $\mathbf{d}$. In theory, a design variable d_k can be any distribution parameter or a statistic; however, here, d_k is limited to the mean of random variable X_k. Many engineering problems related to manufacturing variables, as verified in Refs. [38–40], seek optimal design solutions as the mean values of random variables. If the deterministic parameters are design variables, the resulting problems require additional regularity conditions that describe the differentiability of performance functions with respect to such deterministic parameters [41–44]. The associated sensitivity analysis required for design optimization can be performed without much computational difficulty.

Let $y_l(\mathbf{X}) := y_l(X_1, \ldots, X_N)$, $l = 0, 1, \ldots, K$, represent a collection of $(K+1)$ real-valued, square-integrable, measurable transformations on $(\Omega_{\mathbf{d}}, \mathcal{F}_{\mathbf{d}})$, describing performance functions of a complex system. It is assumed that $y_l : (\mathbb{A}^N, \mathcal{B}^N) \to (\mathbb{R}, \mathcal{B})$ is not an explicit function of $\mathbf{d}$, although y_l implicitly depends on $\mathbf{d}$ via the probability law of $\mathbf{X}$. Also, let $\mathcal{D} = \times_{k=1}^{M}[d_{k,L}, d_{k,R}]$ be a closed rectangular subregion of $\mathbb{R}^M$, where $d_{k,L}$ and $d_{k,U}$ are the lower and upper bounds, respectively, of the kth design variable d_k.

Two mathematical formulations of each RDO and RBDO—one narrated with respect to the original input random variables and the other stated with respect to transformed input random variables—are discussed in the rest of this section. The formulations are equivalent because they lead to matching solutions to a general design optimization problem. However, the latter is more advantageous than the former in light of DD-GPCE approximations, as will be further explained in upcoming sections.

2.1 Original Formulation

Define an objective function $c_0 : \mathcal{D} \to \mathbb{R}$ and constraint functions $c_l : \mathcal{D} \to \mathbb{R}$, where $l = 1, \ldots, K$ and $1 \le K < \infty$.

- RDO

  The mathematical formulation of RDO in most engineering applications requires one to solve [29,45–47]

$$\begin{aligned} \min_{\mathbf{d}\in\mathcal{D}\subseteq\mathbb{R}^M} \quad & c_0(\mathbf{d}) := G\Big(\mathbb{E}_{\mathbf{d}}[y_0(\mathbf{X})],\ \sqrt{\mathrm{var}_{\mathbf{d}}[y_0(\mathbf{X})]}\Big), \\ \text{subject to} \quad & c_l(\mathbf{d}) := \alpha_l\sqrt{\mathrm{var}_{\mathbf{d}}[y_l(\mathbf{X})]} - \mathbb{E}_{\mathbf{d}}[y_l(\mathbf{X})] \le 0, \\ & l = 1, \ldots, K, \\ & d_{k,L} \le d_k \le d_{k,U},\quad k = 1, \ldots, M, \end{aligned} \tag{1}$$

  where

$$\mathbb{E}_{\mathbf{d}}[y_l(\mathbf{X})] := \int_{\mathbb{A}^N} y_l(\mathbf{x}) f_{\mathbf{X}}(\mathbf{x};\mathbf{d}) d\mathbf{x} \tag{2}$$

  is the mean of $y_l(\mathbf{X})$ and

$$\mathrm{var}_{\mathbf{d}}[y_l(\mathbf{x})] := \mathbb{E}_{\mathbf{d}}[y_l(\mathbf{X}) - \mathbb{E}_{\mathbf{d}}[y_l(\mathbf{X})]]^2 \tag{3}$$

  is the variance of $y_l(\mathbf{X})$. Here, $\mathbb{E}_{\mathbf{d}}$ and $\mathrm{var}_{\mathbf{d}}$ are the expectation and variance operators, respectively, with respect to the probability measure $\mathbb{P}_{\mathbf{d}}$ or $f_{\mathbf{X}}(\mathbf{x};\mathbf{d})d\mathbf{x}$ of $\mathbf{X}$; $\alpha_l \in \mathbb{R}_0^+$, $l = 1, \ldots, K$, are non-negative, real-valued constants associated with the probabilities of constraint satisfaction; and $G(\cdot,\cdot)$ is an arbitrary function determined by the choice of scalarization. A commonly used variant of the scalarized objective function is the weighted sum of the first two moments [29,47], yielding

$$\begin{aligned} & G\Big(\mathbb{E}_{\mathbf{d}}[y_0(\mathbf{X})],\ \sqrt{\mathrm{var}_{\mathbf{d}}[y_0(\mathbf{X})]}\Big) \\ & \qquad := w_1\frac{\mathbb{E}_{\mathbf{d}}[y_0(\mathbf{X})]}{\mu_0^*} + w_2\frac{\sqrt{\mathrm{var}_{\mathbf{d}}[y_0(\mathbf{X})]}}{\sigma_0^*}, \end{aligned} \tag{4}$$

where $w_1 \in \mathbb{R}_0^+$ and $w_2 \in \mathbb{R}_0^+$ are two non-negative, real-valued weights such that $w_1 + w_2 = 1$; $\mu_0^* \in \mathbb{R} \setminus \{0\}$ and $\sigma_0^* \in \mathbb{R}_0^+ \setminus \{0\}$ are two non-zero, real-valued scaling factors.

For the scalarization, equal weight values are usually selected, but they can be distinct and biased, depending on the objective set forth by a designer. In contrast, the scaling factors are relatively arbitrary and chosen to achieve better optimal results, for example, by normalizing the objective function.

- RBDO

The mathematical formulation of RBDO requires one to solve [2,8,9]

$$\begin{aligned} \min_{\mathbf{d} \in \mathcal{D} \subseteq \mathbb{R}^M} \quad & c_0(\mathbf{d}), \\ \text{subject to} \quad & c_l(\mathbf{d}) := \mathbb{P}_{\mathbf{d}}[\mathbf{X} \in \Omega_{F,l}(\mathbf{d})] - p_l \leq 0, \\ & l = 1, \ldots, K, \\ & d_{k,L} \leq d_k \leq d_{k,U},\ k = 1, \ldots, M, \end{aligned} \tag{5}$$

where $\Omega_{F,l}(\mathbf{d})$ is the lth failure domain, and $0 \leq p_l \leq 1$ is the lth target failure probability. The objective function c_0 is commonly prescribed as a deterministic function of $\mathbf{d}$, describing relevant system geometry, such as area, volume, and mass. In contrast, the constraint functions c_l, $l = 1, 2, \ldots, K$, are generally more complicated than the objective function. Depending on the failure domain $\Omega_{F,l}$, a component or a system failure probability can be envisioned. For component reliability analysis, the failure domain is often adequately described by a single performance function $y_l(\mathbf{X})$, for instance, $\Omega_{F,l} := \{\mathbf{x} : y_l(\mathbf{x}) < 0\}$, whereas multiple, interdependent performance functions $y_{l,i}(\mathbf{x}),\ i = 1, 2, \ldots$, are required for system reliability analysis, leading, for example, to $\Omega_{F,l} := \cup_i \{\mathbf{x} : y_{l,i}(\mathbf{x}) < 0\}$ and $\Omega_{F,l} := \cap_i \{\mathbf{x} : y_{l,i}(\mathbf{x}) < 0\}$ for series and parallel systems, respectively. Here, $\cup_i$ and $\cap_i$ present a union and intersection, respectively, of the ith components. In either case, the evaluation of the failure probability in Eq. (5) is fundamentally equivalent to calculating a high-dimensional integral over a complex failure domain.

The evaluation of probabilistic constraints $c_l(\mathbf{d})$, $l = 1, 2, \ldots, K$, in RDO and RBDO requires calculating statistical moments and probabilities of failure defined by the corresponding performance functions. A coupling with a gradient-based optimization algorithm demands that the gradients of $c_l(\mathbf{d})$ also be formulated, thus warranting design sensitivity analysis of moments and failure probability.

2.2 Alternative Formulation

Since the design variables are considered as the statistical means of some or all input random variables, a linear transformation, such as the shifting or scaling of random variables, yields alternative formulations of RDO and RBDO. To do so, let $(X_{i_1}, \ldots, X_{i_M})^\intercal$ be an M-dimensional subvector of $\mathbf{X} := (X_1, \ldots, X_N)^\intercal$, $1 \leq i_1 \leq \ldots \leq i_M \leq N$, $M \leq N$, such that the mean of its kth component is the kth design variable, as follows: $\mathbb{E}_{\mathbf{d}}[X_{i_k}] = d_k$, $k = 1, \ldots, M$.

Shifting. Let $\mathbf{Z} := (Z_1, \ldots, Z_N)^\intercal$ be an N-dimensional vector of new random variables obtained by shifting $\mathbf{X}$ as

$$\mathbf{Z} = \mathbf{X} + \mathbf{r}, \tag{6}$$

where $\mathbf{r} := (r_1, \ldots, r_N)^\intercal$ is an N-dimensional vector of deterministic variables. Denote by $(Z_{i_1}, \ldots, Z_{i_M})^\intercal$ a subvector of $\mathbf{Z}$, where the i_kth new random variable Z_{i_k} corresponds to the i_kth original random variable X_{i_k}. Define $g_k := \mathbb{E}_{\mathbf{d}}[Z_{i_k}]$ as the mean of the i_kth component of $\mathbf{Z}$. Then, the mean of Z_{i_k} from the shifting transformation is

$$\mathbb{E}_{\mathbf{d}}[Z_{i_k}] = d_k + r_{i_k} = g_k, \tag{7}$$

and the PDF of $\mathbf{Z}$ is

$$f_{\mathbf{Z}}(\mathbf{z}; \mathbf{g}) = |\mathbf{J}| f_{\mathbf{X}}(\mathbf{x}; \mathbf{d}) = f_{\mathbf{X}}(\mathbf{x}; \mathbf{d}) = f_{\mathbf{X}}(\mathbf{z} - \mathbf{r}; \mathbf{d}), \tag{8}$$

supported on the domain of $\mathbf{Z}$, say, $\bar{\mathbb{A}}^N \subseteq \mathbb{R}^N$. Here, the absolute value of the determinant of the Jacobian matrix is $|\mathbf{J}| = |\det[\partial \mathbf{x}/\partial \mathbf{z}]| = 1$ and the M-dimensional vector $\mathbf{g} := (g_1, \ldots, g_M)^\intercal$ has its kth component such that $g_k = \mathbb{E}_{\mathbf{d}}[Z_{i_k}]$, $k = 1, \ldots, M$.

Scaling. Let $\mathbf{Z} := (Z_1, \ldots, Z_N)^\intercal$ be an N-dimensional vector of new random variables obtained by scaling $\mathbf{X}$ as

$$\mathbf{Z} = \text{diag}[r_1, \ldots, r_N]\mathbf{X}, \tag{9}$$

where $\mathbf{r} := (r_1, \ldots, r_N)^\intercal$ is an N-dimensional vector of deterministic variables. Denote by $(Z_{i_1}, \ldots, Z_{i_M})^\intercal$ a sub-vector of $\mathbf{Z}$, where the i_kth new random variable Z_{i_k} corresponds to the i_kth original random variable X_{i_k}. Define $g_k := \mathbb{E}_{\mathbf{d}}[Z_{i_k}]$ as the mean of the i_kth component of $\mathbf{Z}$. Then, the mean of Z_{i_k} from the scaling transformation is

$$\mathbb{E}_{\mathbf{d}}[Z_{i_k}] = d_k r_{i_k} = g_k, \tag{10}$$

and the PDF of $\mathbf{Z}$ is

$$\begin{aligned} f_{\mathbf{Z}}(\mathbf{z}; \mathbf{g}) &= |\mathbf{J}| f_{\mathbf{X}}(\mathbf{x}; \mathbf{d}) = \left| \frac{1}{r_1 \ldots r_N} \right| f_{\mathbf{X}}(\mathbf{x}; \mathbf{d}) \\ &= \left| \frac{1}{r_1 \ldots r_N} \right| f_{\mathbf{X}}(\text{diag}[1/r_1, \ldots, 1/r_N]\mathbf{z}; \mathbf{d}), \end{aligned} \tag{11}$$

supported on the domain of $\mathbf{Z}$, say, $\bar{\mathbb{A}}^N \subseteq \mathbb{R}^N$. Here, the absolute value of the determinant of the Jacobian matrix is $|\mathbf{J}| = |\det[\partial \mathbf{x}/\partial \mathbf{z}]| = |1/(r_1 \ldots r_N)|$ and the M-dimensional vector $\mathbf{g} := (g_1, \ldots, g_M)^\intercal$ has its kth component such that $g_k = \mathbb{E}_{\mathbf{d}}[Z_{i_k}]$, $k = 1, \ldots, M$.

For each $l = 1, 2, \ldots, K$, define $h_l(\mathbf{Z}; \mathbf{r}) := y_l(\mathbf{X})$ to be the generic output function of the new random variables $\mathbf{Z}$, where the relation between $\mathbf{Z}$ and $\mathbf{X}$ is obtained by either the shifting transformation in Eq. (6) or the scaling transformation in Eq. (9). Correspondingly, a stochastic design optimization, whether RDO or RBDO, can be stated as follows.

- RDO

  In both shifting and scaling cases, the RDO formulation in Eq. (1) is reformulated, yielding [29]

$$\begin{aligned} \min_{\mathbf{d} \in \mathcal{D} \subseteq \mathbb{R}^M} \quad & c_0(\mathbf{d}) := G\Big(\mathbb{E}_{\mathbf{g}(\mathbf{d})}[h_0(\mathbf{Z}; \mathbf{r})],\ \sqrt{\text{var}_{\mathbf{g}(\mathbf{d})}[h_0(\mathbf{Z}; \mathbf{r})]} \Big), \\ \text{subject to} \quad & c_l(\mathbf{d}) := \alpha_l \sqrt{\text{var}_{\mathbf{g}(\mathbf{d})}[h_l(\mathbf{Z}; \mathbf{r})]} - \mathbb{E}_{\mathbf{g}(\mathbf{d})}[h_l(\mathbf{Z}; \mathbf{r})] \leq 0, \\ & \quad l = 1, \ldots, K, \\ & \quad d_{k,L} \leq d_k \leq d_{k,U},\ k = 1, \ldots, M, \end{aligned} \tag{12}$$

  where

$$\mathbb{E}_{\mathbf{g}(\mathbf{d})}[h_l(\mathbf{Z}; \mathbf{r})] := \int_{\bar{\mathbb{A}}^N} h_l(\mathbf{z}; \mathbf{r}) f_{\mathbf{Z}}(\mathbf{z}; \mathbf{g}) d\mathbf{z} \tag{13}$$

  is the mean of $h_l(\mathbf{Z}; \mathbf{r})$ and

$$\text{var}_{\mathbf{g}(\mathbf{d})}[h_l(\mathbf{Z}; \mathbf{r})] := \mathbb{E}_{\mathbf{g}(\mathbf{d})}\big[h_l(\mathbf{Z}; \mathbf{r}) - \mathbb{E}_{\mathbf{g}(\mathbf{d})}[h_l(\mathbf{Z}; \mathbf{r})]\big]^2 \tag{14}$$

  is the variance of $h_l(\mathbf{Z}; \mathbf{r})$. Here, $\mathbb{E}_{\mathbf{g}(\mathbf{d})}$ and $\text{var}_{\mathbf{g}(\mathbf{d})}$ are the expectation and variance operators, respectively, with respect to the probability measure $f_{\mathbf{Z}}(\mathbf{z}; \mathbf{g})d\mathbf{z}$, which depends on $\mathbf{g}$. For brevity, the subscript "$\mathbf{g}(\mathbf{d})$" of the expectation operator will be denoted by "$\mathbf{g}$" in the rest of the paper.

- RBDO

  In both shifting and scaling cases, the RBDO formulation in Eq. (5) is reformulated, yielding [9]

$$\begin{aligned} \min_{\mathbf{d}\in\mathcal{D}\subseteq\mathbb{R}^M} \quad & c_0(\mathbf{d}), \\ \text{subject to} \quad & c_l(\mathbf{d}) := \mathbb{P}_{\mathbf{g(d)}}[\mathbf{Z}\in\bar{\Omega}_{F,l}(\mathbf{d})] - p_l \le 0, \\ & l = 1,\dots,K, \\ & d_{k,L} \le d_k \le d_{k,U},\ k = 1,\dots,M, \end{aligned} \tag{15}$$

  where $\bar{\Omega}_{F,l}(\mathbf{d})$ is the lth failure domain such that $\bar{\Omega}_{F,l} := \{\mathbf{z} : h_l(\mathbf{z};\mathbf{r}) < 0\}$ for component reliability analysis of a performance function $h_l(\mathbf{z};\mathbf{r})$, and $\bar{\Omega}_{F,l} := \cup_i\{\mathbf{z} : h_{l,i}(\mathbf{z};\mathbf{r}) < 0\}$ or $\cap_i\{\mathbf{z} : h_{l,i}(\mathbf{z};\mathbf{r}) < 0\}$ if at least two performance functions $h_{l,i}(\mathbf{z};\mathbf{r}),\ i = 1,2,\dots,$ are involved in series or parallel systems, respectively, for system reliability analysis.

  The alternative formulations in Eqs. (12) and (15) are the restatement of Eqs. (1) and (5), respectively, with respect to the transformed input random variables $\mathbf{Z}$. In these alternative formulations, the probability measure of $\mathbf{Z}$ is locked during design iterations, thus sidestepping the need to recalculate measure-associated quantities. For the remainder of the paper, the solutions of RDO and RBDO problems will be reported with respect to the alternative formulation. Furthermore, $\mathbf{X}$ or $\mathbf{Z}$ and y_l or h_l will be referred to, interchangeably, as input random vector and output function, respectively.

A gradient-based optimization solution to the RDO or RBDO problem in Eq. (12) or Eq. (15), respectively, mandates adequate smoothness of objective and constraint functions. Therefore, these functions are assumed to be differentiable with respect to design variables. Usually, the optimal solution of Eqs. (12) and (15) can be determined by a suitable programming method, such as the sequential linear or quadratic programming methods.

3. DIMENSIONALLY DECOMPOSED GENERALIZED POLYNOMIAL CHAOS EXPANSION

Given an input random vector $\mathbf{X} := (X_1,\dots,X_N)^\intercal$ or its transformed version $\mathbf{Z} := (Z_1,\dots,Z_N)^\intercal$ with known PDF $f_{\mathbf{X}}(\mathbf{x};\mathbf{d})$ or $f_{\mathbf{Z}}(\mathbf{z};\mathbf{g})$, let $h(\mathbf{Z};\mathbf{r})$ represent any one of the random output functions $h_0(\mathbf{Z};\mathbf{r})$ and $h_l(\mathbf{Z};\mathbf{r})$, $l = 1,\dots,K$, in Eqs. (12) and (15). Here, $h(\mathbf{Z};\mathbf{r})$ is assumed to belong to a reasonably large class of random variables, such as the Hilbert space:

$$L^2(\Omega_{\mathbf{d}},\mathcal{F}_{\mathbf{d}},\mathbb{P}_{\mathbf{d}}) := \left\{h : \Omega_{\mathbf{d}} \to \mathbb{R} : \int_{\Omega_{\mathbf{d}}} h^2(\mathbf{Z};\mathbf{r})d\mathbb{P}_{\mathbf{d}} < \infty\right\}. \tag{16}$$

This is analogous to saying that the real-valued function $h(\mathbf{z};\mathbf{r})$ lives in the equivalent Hilbert space:

$$\left\{h : \bar{\mathbb{A}}^N \to \mathbb{R} : \int_{\bar{\mathbb{A}}^N} h^2(\mathbf{z};\mathbf{r}) f_{\mathbf{Z}}(\mathbf{z};\mathbf{g})d\mathbf{z} < \infty\right\}. \tag{17}$$

When $\mathbf{Z} = (Z_1,\dots,Z_N)^\intercal$ comprises statistically dependent random variables, the resultant probability measure, in general, is not a product type, meaning that the joint distribution of $\mathbf{Z}$ cannot be obtained strictly from its marginal distributions. Consequently, measure-consistent multivariate orthonormal polynomials in $\mathbf{z} = (z_1,\dots,z_N)^\intercal$ cannot be built from an N-dimensional tensor product of measure-consistent univariate orthonormal polynomials. In this case, a three-step algorithm founded on a whitening transformation of the monomial basis can be employed to determine multivariate orthonormal polynomials consistent with an arbitrary, non-product-type probability measure $f_{\mathbf{Z}}(\mathbf{z};\mathbf{g})d\mathbf{z}$ of $\mathbf{Z}$.

Appendix A briefly summarizes GPCE that expands any output random variable $h(\mathbf{Z}) \in L^2(\Omega_{\mathbf{d}},\mathcal{F}_{\mathbf{d}},\mathbb{P}_{\mathbf{d}})$ into a Fourier series comprising measure-consistent multivariate orthonormal polynomials. The truncated GPCE in Appendix A is referred to as *regular* GPCE in this work.

3.1 Construction of DD-GPCE

For truly high-dimensional problems, the aforementioned regular GPCE approximation requires an astronomically large number of basis functions or coefficients, thus succumbing to the curse of dimensionality. However, in many real-world applications, high-variate interaction effects among input variables are often negligible to the output function value of interest. In this section, a DD-GPCE approximation, reorganizing the basis functions of regular GPCE in a dimensionwise manner, is introduced for the first time. The DD-GPCE has an ability to safely and effectively select the basis functions or coefficients of the regular GPCE further in terms of degree of interaction among input variables, thereby tackling the curse of dimensionality to some extent. The chosen multivariate orthonormal polynomials that are consistent with an arbitrary, non-product-type probability measure $f_{\mathbf{Z}}(\mathbf{z};\mathbf{g})d\mathbf{z}$ of $\mathbf{Z}$ are determined by the three-step algorithm founded on a whitening transformation of the monomial basis as follows.

3.1.1 Monomial Basis

For $N \in \mathbb{N}$, denote by $\{1,\ldots,N\}$ an index set, so that $u \subseteq \{1,\ldots,N\}$ is a subset, including the empty set $\emptyset$, with cardinality $0 \le |u| \le N$. The complementary subset of u is denoted by $-u := \{1,\ldots,N\}\backslash u$. For each $m \in \mathbb{N}_0$ and $0 \le S \le N$, consider the elements of the reduced multi-index set,

$$\mathcal{J}_{S,m} := \Big\{\mathbf{j} = (\mathbf{j}_u, \mathbf{0}_{-u}) \in \mathbb{N}_0^N : \mathbf{j}_u \in \mathbb{N}^{|u|},\ |u| \le |\mathbf{j}_u| \le m,\ 0 \le |u| \le S\Big\},\ \ |\mathbf{j}_u| := j_{i_1} + \ldots + j_{i_{|u|}},$$

which is arranged as $\mathbf{j}^{(1)},\ldots,\mathbf{j}^{(L_{N,S,m})}$, $\mathbf{j}^{(1)} = \mathbf{0}$, according to a monomial order of choice. Here, $(\mathbf{j}_u, \mathbf{0}_{-u})$ denotes an N-dimensional multi-index whose ith component is j_i if $i \in u$ and 0 if $i \notin u$. It is elementary to show that the $\mathcal{J}_{S,m}$ has cardinality $L_{N,S,m}$, given by

$$L_{N,S,m} := |\mathcal{J}_{S,m}| = 1 + \sum_{s=1}^{S} \binom{N}{s}\binom{m}{s} \le L_{N,m}, \tag{18}$$

where $L_{N,m}$ is the cardinality of the multi-index set $\mathcal{J}_m$ for the regular GPCE, which is also defined in Appendix A. Here, $\mathcal{J}_{S,m}$ represents a subset of $\mathcal{J}_m$, determined from the chosen S relevant for the DD-GPCE. Denote by

$$\mathbf{P}_{S,m}(\mathbf{z}) = \left(\mathbf{z}^{\mathbf{j}^{(1)}},\ldots,\mathbf{z}^{\mathbf{j}^{(L_{N,S,m})}}\right)^{\intercal}$$

an $L_{N,S,m}$-dimensional column vector where the elements are the monomials $\mathbf{z}^{\mathbf{j}}$ for $\mathbf{j} \in \mathcal{J}_{S,m}$ arranged in the aforementioned order. For $u \subseteq \{1,\ldots,N\}$, let $\mathbf{z}_u := (z_{i_1},\ldots,z_{i_{|u|}})^{\intercal}$, $1 \le i_1 < \ldots < i_{|u|} \le N$, be a subvector of $\mathbf{z}$. The complementary subvector is defined by $\mathbf{z}_{-u} := \mathbf{z}_{\{1,\ldots,N\}\backslash u}$. Then, for $\mathbf{j} \in \mathcal{J}_{S,m}$,

$$\mathbf{z}^{\mathbf{j}} = \mathbf{z}_u^{\mathbf{j}_u}\mathbf{0}_{-u}{}^{\mathbf{j}_{-u}} = \mathbf{z}_u^{\mathbf{j}_u}.$$

Therefore, $\mathbf{P}_{S,m}(\mathbf{z})$ is the monomial vector in $\mathbf{z}_u = (z_{i_1},\ldots,z_{i_{|u|}})^{\intercal}$ of degree $0 \le |u| \le S$ and $|u| \le |\mathbf{j}_u| \le m$.

3.1.2 Monomial Moment Matrix

When the input random variables $Z_1,\ldots,Z_N$, instead of the real variables $z_1,\ldots,z_N$, are inserted in the argument, $\mathbf{P}_{S,m}(\mathbf{Z})$ becomes a vector of random monomials. This leads to an $L_{N,S,m} \times L_{N,S,m}$ monomial moment matrix of $\mathbf{P}_{S,m}(\mathbf{Z})$, defined as

$$\mathbf{G}_{S,m} := \mathbb{E}_{\mathbf{g}}[\mathbf{P}_{S,m}(\mathbf{Z})\mathbf{P}_{S,m}^{\intercal}(\mathbf{Z})] := \int_{\bar{\mathbb{A}}^N} \mathbf{P}_{S,m}(\mathbf{z})\mathbf{P}_{S,m}^{\intercal}(\mathbf{z}) f_{\mathbf{Z}}(\mathbf{z};\mathbf{g})d\mathbf{z}, \tag{19}$$

with its (p,q)th element

$$G_{S,m,pq} := \mathbb{E}_{\mathbf{g}}[\mathbf{Z}^{\mathbf{j}^{(p)}}\mathbf{Z}^{\mathbf{j}^{(q)}}] := \int_{\bar{\mathbb{A}}^N} \mathbf{z}^{\mathbf{j}^{(p)}}\mathbf{z}^{\mathbf{j}^{(q)}} f_{\mathbf{Z}}(\mathbf{z};\mathbf{g})d\mathbf{z} = \int_{\bar{\mathbb{A}}^N} \mathbf{z}^{\mathbf{j}^{(p)}+\mathbf{j}^{(q)}} f_{\mathbf{Z}}(\mathbf{z};\mathbf{g})d\mathbf{z},\ \ p,q = 1,\ldots,L_{N,S,m}. \tag{20}$$

When $0 \leq S \leq N$ and $S \leq m < \infty$, $G_{S,m,pq}$ represents the expectation of a product of two random monomials $\mathbf{Z}^{\mathbf{j}^{(p)}}$ and $\mathbf{Z}^{\mathbf{j}^{(q)}}$, where $\mathbf{j}^{(p)}$ and $\mathbf{j}^{(q)}$ are the pth and qth elements, respectively, of $\mathcal{J}_{S,m}$ in the aforementioned order. For $u, v \subseteq \{1, \ldots, N\}$, $0 \leq |u|, |v| \leq S$, $\mathbf{z}^{\mathbf{j}^{(p)}} = \mathbf{z}_u^{\mathbf{j}_u}$ and $\mathbf{z}^{\mathbf{j}^{(q)}} = \mathbf{z}_v^{\mathbf{j}_v}$, yielding

$$G_{S,m,pq} := \int_{\bar{\mathbb{A}}^{|u \cup v|}} \mathbf{z}_u^{\mathbf{j}_u} \mathbf{z}_v^{\mathbf{j}_v} f_{\mathbf{Z}_{u \cup v}}(\mathbf{z}_{u \cup v}; \mathbf{g}) d\mathbf{z}_{u \cup v}, \;\; p, q = 1, \ldots, L_{N,S,m}. \tag{21}$$

Here, $\mathbf{z}_{u \cup v} = (z_{i_1}, \ldots, z_{i_{|u \cup v|}})^\intercal$, $1 \leq i_1 < \ldots < i_{|u \cup v|} \leq N$ of a subvector of $\mathbf{z}$. Therefore, the calculation of a monomial moment matrix demands the $|u \cup v|$-dimensional integration. When compared with the monomial moment matrix $\mathbf{G}_m$ in Eq. (A.4) from Appendix A, the merit in calculating $\mathbf{G}_{S,m}$ in Eq. (19) can be significant in terms of the computational cost. For example, if $N = 10$, and $m = 10$, the calculation of $\mathbf{G}_{S,m}$ with $S = 1$ requires at most two-dimensional integration with respect to a bivariate marginal distribution. In contrast, the calculation of $\mathbf{G}_m$, whose (p, q)th elements are

$$G_{m,pq} := \int_{\bar{\mathbb{A}}^N} \mathbf{z}^{\mathbf{j}^{(p)} + \mathbf{j}^{(q)}} f_{\mathbf{Z}}(\mathbf{z}; \mathbf{g}) d\mathbf{z}, \;\; p, q = 1, \ldots, L_{N,m}, \tag{22}$$

requires at most ten-dimensional integration with respect to a decavariate joint distribution. Moreover, such high-dimensional joint distribution in the latter is more difficult to obtain than its lower-dimensional or marginal version or may not be possible to obtain when the type of probability distribution is arbitrary or unknown.

It is elementary to show that $\mathbf{G}_{S,m}$ is symmetric and positive-definite. Therefore, $\mathbf{G}_{S,m}$ is invertible, facilitating a whitening transformation, to be discussed next.

3.1.3 Whitening Transformation

Given $0 \leq S \leq N$, $S \leq m < \infty$, and the previously chosen monomial order, denote by

$$\boldsymbol{\Psi}_{S,m}(\mathbf{z}; \mathbf{g}) := (\Psi_{\mathbf{j}^{(1)}}(\mathbf{z}; \mathbf{g}), \ldots, \Psi_{\mathbf{j}^{(L_{N,S,m})}}(\mathbf{z}; \mathbf{g}))^\intercal := (\Psi_1(\mathbf{z}; \mathbf{g}), \ldots, \Psi_{L_{N,S,m}}(\mathbf{z}; \mathbf{g}))^\intercal \tag{23}$$

an $L_{N,S,m}$-dimensional column vector of orthonormal polynomials, which is consistent with the probability measure $f_{\mathbf{Z}}(\mathbf{z}; \mathbf{g})d\mathbf{z}$. Such polynomials can be generated from the monomial vector $\mathbf{P}_{S,m}$ and properties of the monomial moment matrix $\mathbf{G}_{S,m}$. In Eq. (23), $\Psi_{\mathbf{j}^{(p)}}(\mathbf{z}; \mathbf{g})$, $p = 1, \ldots, L_{N,S,m}$, represents the pth element of $\boldsymbol{\Psi}_{S,m}(\mathbf{z}; \mathbf{g})$ consistent with the monomial order of choice, whereas, for simplicity, the subscript $\mathbf{j}^{(p)}$ has been replaced with p in the second equality to denote the same element. To construct such orthonormal polynomials, recognize that the monomial moment matrix $\mathbf{G}_{S,m}$, as it is symmetric and positive-definite, is invertible. Therefore, for $0 \leq S \leq N$ and $S \leq m < \infty$, there exists a nonsingular $L_{N,S,m} \times L_{N,S,m}$ whitening matrix $\mathbf{W}_{S,m}$, satisfying

$$\mathbf{W}_{S,m}^\intercal \mathbf{W}_{S,m} = \mathbf{G}_{S,m}^{-1} \;\text{ or }\; \mathbf{W}_{S,m}^{-1} \mathbf{W}_{S,m}^{-\intercal} = \mathbf{G}_{S,m}. \tag{24}$$

Thereafter, apply a whitening transformation to create the orthonormal polynomial vector,

$$\boldsymbol{\Psi}_{S,m}(\mathbf{z}; \mathbf{g}) = \mathbf{W}_{S,m} \mathbf{P}_{S,m}(\mathbf{z}), \tag{25}$$

from the known monomial vector $\mathbf{P}_{S,m}(\mathbf{z})$. The whitening matrix $\mathbf{W}_{S,m}$ involved in Eq. (24) is not uniquely determined from the invertibility of $\mathbf{G}_{S,m}$. Indeed, there are multiple options to select $\mathbf{W}_{S,m}$, all fulfilling the condition described in Eq. (24).

A prominent choice of the whitening matrix involves Cholesky factorization [32], which leads to the following selection of

$$\mathbf{W}_{S,m} = \mathbf{Q}_{S,m}^{-1}, \;\; \mathbf{G}_{S,m} = \mathbf{Q}_{S,m} \mathbf{Q}_{S,m}^\intercal. \tag{26}$$

Here, $\mathbf{Q}_{S,m}$ is an $L_{N,S,m} \times L_{N,S,m}$ real-valued lower-triangular matrix determined from the Cholesky factorization of $\mathbf{G}_{S,m}$. Interested readers are encouraged to review the prior work [32] on additional choices for the whitening matrix.

It is important not to confuse the whitening transformation with measure transformations frequently used for mapping dependent variables to independent ones. The latter transformations are generally nonlinear for non-Gaussian variables. In contrast, the transformation introduced here is linear and maps monomials to orthonormal polynomials for any input probability measure. As long as the monomial moment matrix $\mathbf{G}_{S,m}$ exists and can be constructed, as discussed more in a forthcoming subsection, orthonormal polynomials consistent with a wide variety of dependent variables can be created.

Finally, for $i, j = 1, \ldots, L_{N,S,m}$, the ith and jth elements of the polynomial vector $\mathbf{\Psi}_{S,m}(\mathbf{z};\mathbf{g})$ also have the first- and second-order moments, satisfying Eqs. (A.7) and (A.8), respectively.

Note that these orthonormal polynomials are described in terms of **z**, not **x**. This is mainly because **g** and hence $\mathbf{\Psi}_m(\mathbf{z};\mathbf{g})$ are desired to be invariant when the design vector **d** is updated during design iterations. Readers interested in further details should review prior works of the authors [9,29].

3.1.4 An Illustrative Example

From the general three-step algorithm just described, a specific yet clarifying example in generating orthonormal polynomials for DD-GPCE and regular GPCE would be illuminating. For instance, consider two ($N = 2$) statistically dependent *zero*-mean Gaussian random variables Z_1 and Z_2 with identical standard deviations $\sigma_1 = \sigma_2 = 1/4$ and correlation coefficient $\rho = 9/10$.

Case 1: Set $S = 1$ and $m = 3$ to generate at most univariate, third-order measure-consistent orthonormal polynomials in $\mathbf{z} = (z_1, z_2)^\intercal \in \mathbb{R}^2$ of DD-GPCE.

From Eq. (18), $L_{2,1,3} = 1 + \sum_{s=1}^{1} \binom{2}{s}\binom{3}{s} = 7$. Hence, the reduced multi-index set and the monomial vector are

$$\mathcal{J}_{1,3} = \{(0,0),(1,0),(0,1),(2,0),(0,2),(3,0),(0,3)\},$$

$$\mathbf{P}_{1,3}(z_1, z_2) = (1, z_1, z_2, z_1^2, z_2^2, z_1^3, z_2^3)^\intercal.$$

Using Eqs. (19) and (26), the monomial moment matrix and whitening matrix are exactly calculated as

$$\mathbf{G}_{1,3} = \begin{bmatrix} 1 & 0 & 0 & \frac{1}{16} & \frac{1}{16} & 0 & 0 \\ 0 & \frac{1}{16} & \frac{9}{160} & 0 & 0 & \frac{3}{256} & \frac{27}{2560} \\ 0 & \frac{9}{160} & \frac{1}{16} & 0 & 0 & \frac{27}{2560} & \frac{3}{256} \\ \frac{1}{16} & 0 & 0 & \frac{3}{256} & \frac{131}{12{,}800} & 0 & 0 \\ \frac{1}{16} & 0 & 0 & \frac{131}{12{,}800} & \frac{3}{256} & 0 & 0 \\ 0 & \frac{3}{256} & \frac{27}{2560} & 0 & 0 & \frac{15}{4096} & \frac{6237}{2{,}048{,}000} \\ 0 & \frac{27}{2560} & \frac{3}{256} & 0 & 0 & \frac{6237}{2{,}048{,}000} & \frac{15}{4096} \end{bmatrix},$$

$$\mathbf{W}_{1,3} = \begin{bmatrix} 1 & 0 & 0 & 0 & 0 & 0 & 0 \\ 0 & 4 & 0 & 0 & 0 & 0 & 0 \\ 0 & -\frac{36}{\sqrt{19}} & \frac{40}{\sqrt{19}} & 0 & 0 & 0 & 0 \\ -\frac{1}{\sqrt{2}} & 0 & 0 & 8\sqrt{2} & 0 & 0 & 0 \\ -\sqrt{\frac{19}{362}} & 0 & 0 & -648\sqrt{\frac{2}{3439}} & 800\sqrt{\frac{2}{3439}} & 0 & 0 \\ 0 & -2\sqrt{6} & 0 & 0 & 0 & 32\sqrt{\frac{2}{3}} & 0 \\ 0 & 1458\sqrt{\frac{6}{468{,}559}} & -2000\sqrt{\frac{6}{468{,}559}} & 0 & 0 & -7776\sqrt{\frac{6}{468{,}559}} & 32000\sqrt{\frac{2}{1{,}405{,}677}} \end{bmatrix}.$$

Thereafter, Eq. (25) yields an orthonormal polynomial vector as

$$\boldsymbol{\Psi}_{1,3}(z_1,z_2)=\begin{pmatrix} 1 \\ 4z_1 \\ \frac{40z_2}{\sqrt{19}}-\frac{36z_1}{\sqrt{19}} \\ 8\sqrt{2}z_1^2-\frac{1}{\sqrt{2}} \\ -648\sqrt{\frac{2}{3439}}z_1^2+800\sqrt{\frac{2}{3439}}z_2^2-\sqrt{\frac{19}{362}} \\ 32\sqrt{\frac{2}{3}}z_1^3-2\sqrt{6}z_1 \\ -7776\sqrt{\frac{6}{468{,}559}}z_1^3+1458\sqrt{\frac{6}{468{,}559}}z_1+32{,}000\sqrt{\frac{2}{1{,}405{,}677}}z_2^3-2000\sqrt{\frac{6}{468{,}559}}z_2 \end{pmatrix}.$$

Case 2: In reference to Appendix A, set $m=3$ to generate at most third-order measure-consistent orthonormal polynomials in $\mathbf{z}=(z_1,z_2)^\intercal\in\mathbb{R}^2$ of regular GPCE.

From Eq. (A.1), $L_{2,3}=\binom{2+3}{3}=10$. Hence, the unreduced total-degree multi-index set and the monomial vector are

$$\mathcal{J}_3=\{(0,0),(1,0),(0,1),(2,0),(0,2),(3,0),(0,3),(1,1),(2,1),(1,2)\},$$
$$\mathbf{P}_3(z_1,z_2)=(1,z_1,z_2,z_1^2,z_2^2,z_1^3,z_2^3,z_1z_2,z_1^2z_2,z_1z_2^2)^\intercal.$$

Using Eqs. (A.4) and (A.5), the monomial moment matrix and whitening matrix are exactly calculated as

$$\mathbf{G}_3=\begin{bmatrix} 1 & 0 & 0 & \frac{1}{16} & \frac{1}{16} & 0 & 0 & \frac{9}{160} & 0 & 0 \\ 0 & \frac{1}{16} & \frac{9}{160} & 0 & 0 & \frac{3}{256} & \frac{27}{2560} & 0 & \frac{27}{2560} & \frac{131}{12{,}800} \\ 0 & \frac{9}{160} & \frac{1}{16} & 0 & 0 & \frac{27}{2560} & \frac{3}{256} & 0 & \frac{131}{12{,}800} & \frac{27}{2560} \\ \frac{1}{16} & 0 & 0 & \frac{3}{256} & \frac{131}{12{,}800} & 0 & 0 & \frac{27}{2560} & 0 & 0 \\ \frac{1}{16} & 0 & 0 & \frac{131}{12{,}800} & \frac{3}{256} & 0 & 0 & \frac{27}{2560} & 0 & 0 \\ 0 & \frac{3}{256} & \frac{27}{2560} & 0 & 0 & \frac{15}{4096} & \frac{6237}{2{,}048{,}000} & 0 & \frac{27}{8192} & \frac{159}{51{,}200} \\ 0 & \frac{27}{2560} & \frac{3}{256} & 0 & 0 & \frac{6237}{2{,}048{,}000} & \frac{15}{4096} & 0 & \frac{159}{51{,}200} & \frac{27}{8192} \\ \frac{9}{160} & 0 & 0 & \frac{27}{2560} & \frac{27}{2560} & 0 & 0 & \frac{131}{12{,}800} & 0 & 0 \\ 0 & \frac{27}{2560} & \frac{131}{12{,}800} & 0 & 0 & \frac{27}{8192} & \frac{159}{51200} & 0 & \frac{159}{51{,}200} & \frac{6237}{2{,}048{,}000} \\ 0 & \frac{131}{12{,}800} & \frac{27}{2560} & 0 & 0 & \frac{159}{51{,}200} & \frac{27}{8192} & 0 & \frac{6237}{2{,}048{,}000} & \frac{159}{51{,}200} \end{bmatrix},$$

$$\mathbf{W}_3=\begin{bmatrix} 1 & 0 & 0 & 0 & 0 & 0 & 0 & 0 & 0 & 0 \\ 0 & 4 & 0 & 0 & 0 & 0 & 0 & 0 & 0 & 0 \\ 0 & -\frac{36}{\sqrt{19}} & \frac{40}{\sqrt{19}} & 0 & 0 & 0 & 0 & 0 & 0 & 0 \\ -\frac{1}{\sqrt{2}} & 0 & 0 & 8\sqrt{2} & 0 & 0 & 0 & 0 & 0 & 0 \\ -\sqrt{\frac{19}{362}} & 0 & 0 & -648\sqrt{\frac{2}{3439}} & 800\sqrt{\frac{2}{3439}} & 0 & 0 & 0 & 0 & 0 \\ 0 & -2\sqrt{6} & 0 & 0 & 0 & 32\sqrt{\frac{2}{3}} & 0 & 0 & 0 & 0 \\ 0 & 1458\sqrt{\frac{6}{468{,}559}} & -2000\sqrt{\frac{6}{468{,}559}} & 0 & 0 & -7776\sqrt{\frac{6}{468{,}559}} & 32{,}000\sqrt{\frac{2}{1{,}405{,}677}} & 0 & 0 & 0 \\ \frac{9}{\sqrt{181}} & 0 & 0 & -\frac{14{,}400}{19\sqrt{181}} & -\frac{14{,}400}{19\sqrt{181}} & 0 & 0 & \frac{160\sqrt{181}}{19} & 0 & 0 \\ 0 & 36\sqrt{\frac{131}{24{,}661}} & -\frac{380}{\sqrt{3{,}230{,}591}} & 0 & 0 & -\frac{5{,}212{,}800}{19\sqrt{3{,}230{,}591}} & -\frac{2{,}592{,}000}{19\sqrt{3{,}230{,}591}} & 0 & \frac{320\sqrt{\frac{24{,}661}{131}}}{19} & 0 \\ 0 & -4\sqrt{\frac{131}{19}} & \frac{540}{\sqrt{2489}} & 0 & 0 & \frac{259{,}200}{19\sqrt{2489}} & -\frac{288{,}000}{19\sqrt{2489}} & 0 & -\frac{809{,}280}{19\sqrt{2489}} & \frac{6400\sqrt{\frac{131}{19}}}{19} \end{bmatrix}.$$

Thereafter, Eq. (A.6) yields an orthonormal polynomial vector as

$$\boldsymbol{\Psi}_3(z_1,z_2)=\begin{pmatrix} 1 \\ 4z_1 \\ \frac{40z_2}{\sqrt{19}}-\frac{36z_1}{\sqrt{19}} \\ 8\sqrt{2}z_1^2-\frac{1}{\sqrt{2}} \\ -648\sqrt{\frac{2}{3439}}z_1^2+800\sqrt{\frac{2}{3439}}z_2^2-\sqrt{\frac{19}{362}} \\ 32\sqrt{\frac{2}{3}}z_1^3-2\sqrt{6}z_1 \\ -7776\sqrt{\frac{6}{468{,}559}}z_1^3+1458\sqrt{\frac{6}{468{,}559}}z_1+32{,}000\sqrt{\frac{2}{1{,}405{,}677}}z_2^3-2000\sqrt{\frac{6}{468{,}559}}z_2 \\ -\frac{144}{19}\sqrt{181}z_1^2+\frac{11{,}664z_1^2}{19\sqrt{181}}+\frac{160}{19}\sqrt{181}z_2z_1-\frac{14{,}400z_2^2}{19\sqrt{181}}+\frac{9}{\sqrt{181}} \\ -\frac{288}{19}\sqrt{\frac{24{,}661}{131}}z_1^3+\frac{1{,}889{,}568z_1^3}{19\sqrt{3{,}230{,}591}}+\frac{320}{19}\sqrt{\frac{24{,}661}{131}}z_2z_1^2+\frac{18}{19}\sqrt{\frac{24{,}661}{131}}z_1-\frac{354{,}294z_1}{19\sqrt{3{,}230{,}591}}-\frac{2{,}592{,}000z_2^3}{19\sqrt{3{,}230{,}591}}-\frac{20}{19}\sqrt{\frac{24{,}661}{131}}z_2+\frac{486{,}000z_2}{19\sqrt{3{,}230{,}591}} \\ -\frac{51{,}840{,}000\sqrt{\frac{131}{19}}z_1^3}{468{,}559}+\frac{13{,}183{,}171{,}200z_1^3}{468{,}559\sqrt{2489}}-\frac{809{,}280z_2z_1^2}{19\sqrt{2489}}+\frac{6400}{19}\sqrt{\frac{131}{19}}z_2^2z_1-4\sqrt{\frac{131}{19}}z_1-\frac{104{,}256{,}000\sqrt{\frac{131}{19}}z_2^3}{468{,}559}+\frac{6{,}555{,}168{,}000z_2^3}{468{,}559\sqrt{2489}}+\frac{50{,}580\sqrt{\frac{19}{131}}z_2}{24{,}661}+\frac{94{,}320\sqrt{\frac{131}{19}}z_2}{24{,}661} \end{pmatrix}.$$

In Case 1, the truncation of $S = 1$ and $m = 3$ in DD-GPCE requires $L_{2,1,3} = 7$ basis functions, while in Case 2, the truncation of $m = 3$ in regular GPCE mandates $L_{2,3} = 10$ basis functions. The basis functions of the former form a subset of basis functions of the latter. More importantly, DD-GPCE involves fewer basis functions than regular GPCE. The difference in the number of basis functions, while not meaningfully large for only two variables, can be enormous as N increases. For example, when $N = 20$, $S = 1$, and $m = 3$, then the number of regular GPCE's basis functions jumps to 1771, whereas the number of DD-GPCE's basis functions stands at only 61. Similar examples can be given for higher-variate ($S < N$) truncations when N is large. Therefore, DD-GPCE is markedly more effective than regular GPCE in dealing with high-dimensional UQ and design optimization problems, provided that a lower-variate truncation is adequate for calculating the statistical properties of output performance functions. This is the principal motivation behind pursuing the DD-GPCE approximation, which will be formally defined in the following section.

Whether using the regular GPCE or DD-GPCE, it is elementary to verify that their orthonormal polynomials satisfy the statistical properties described in Eqs. (A.7) and (A.8). In general, measure-consistent orthonormal polynomials cannot be determined exactly for an arbitrary probability measure. In such a case, they can be obtained numerically and hence approximately using a Gauss-quadrature method or sampling method. Readers interested in further details should consult the prior work [33].

3.2 DD-GPCE Approximation

A DD-GPCE approximation, dictated by truncation parameters $m \le S \le N$ and $S \le m < \infty$, retains the degree of interaction among input variables less than or equal to S and preserves polynomial orders less than or equal to m. The result is an S-variate, mth-order DD-GPCE approximation

$$h_{S,m}(\mathbf{Z};\mathbf{r}) = \sum_{i=1}^{L_{N,S,m}} C_i(\mathbf{r})\Psi_i(\mathbf{Z};\mathbf{g}) \tag{27}$$

of $h(\mathbf{Z};\mathbf{r})$, which contains expansion coefficients $C_i \in \mathbb{R},\ i = 1,\ldots,L_{N,S,m}$, defined by

$$\begin{aligned} C_i(\mathbf{r}) &:= \mathbb{E}_{\mathbf{g}}[h(\mathbf{Z};\mathbf{r})\Psi_i(\mathbf{Z};\mathbf{g})] \\ &:= \int_{\mathbb{A}^N} h(\mathbf{z};\mathbf{r})\Psi_i(\mathbf{z};\mathbf{g})f_{\mathbf{Z}}(\mathbf{z};\mathbf{g})d\mathbf{z}. \end{aligned} \tag{28}$$

Appendix B summarizes the estimation of expansion coefficients of DD-GPCE via standard least-squares (SLS).

The DD-GPCE presented here entails arbitrarily truncating the GPCE expansion. A more rational or automatic approach to truncate the expansion based on the anisotropy, degree of interaction, and other features of objective and constraint functions will require an adaptive approach, controlled by user-defined error thresholds. The amount of work required to develop such adaptivity is nontrivial, outside the scope of the present work, and currently being studied in the authors' group.

3.3 Stochastic Analysis

The S-variate, mth-order DD-GPCE approximation $h_{S,m}(\mathbf{Z};\mathbf{r})$ can be viewed as an inexpensive surrogate of an expensive-to-calculate function $h(\mathbf{Z};\mathbf{r})$. Therefore, relevant statistical properties of $h(\mathbf{Z};\mathbf{r})$, such as its first two moments and failure probability, can be estimated from those of $h_{S,m}(\mathbf{Z};\mathbf{r})$.

3.3.1 Statistical Moments

Applying the expectation operator on $h_{S,m}(\mathbf{Z};\mathbf{r})$ in Eq. (27) and recognizing Eq. (A.7), its mean

$$\mathbb{E}_{\mathbf{g}}[h_{S,m}(\mathbf{Z};\mathbf{r})] = C_1(\mathbf{r}) = \mathbb{E}_{\mathbf{g}}[h(\mathbf{Z};\mathbf{r})] \tag{29}$$

matches the exact mean of $h(\mathbf{Z};\mathbf{r})$ for $0 \le S \le N$ and $S \le m < \infty$. Enforcing the expectation operator again, this time on $(h_{S,m}(\mathbf{Z};\mathbf{r}) - \mathbb{E}_{\mathbf{g}(\mathbf{d})}[h_{S,m}(\mathbf{Z};\mathbf{r})])^2$, and using Eq. (A.8) results in the variance

$$\begin{aligned} \mathrm{var}_{\mathbf{g}}[h_{S,m}(\mathbf{Z};\mathbf{r})] &= \sum_{i=1}^{L_{N,S,m}} C_i^2(\mathbf{r}) - C_1^2(\mathbf{r}) \\ &= \sum_{i=2}^{L_{N,S,m}} C_i^2(\mathbf{r}) \le \mathrm{var}_{\mathbf{g}}[h(\mathbf{Z};\mathbf{r})] \end{aligned} \tag{30}$$

of $h_{S,m}(\mathbf{Z};\mathbf{r})$, where the equality before the last term operates when $S = N$ and $m \to \infty$. Therefore, the second-moment statistics of a DD-GPCE approximation are solely determined by an appropriately truncated set of expansion coefficients.

3.3.2 Failure Probability

For reliability analysis of performance functions $h(\mathbf{Z};\mathbf{r})$ in Section 2, the estimation of the failure probability can be conducted using MCS of $h_{S,m}(\mathbf{Z};\mathbf{r})$, as follows.

Depending on component or system reliability analysis, let $\bar{\Omega}_{F,S,m} := \{\mathbf{z} : h_{S,m}(\mathbf{z};\mathbf{r}) < 0\}$ or $\bar{\Omega}_{F,S,m} := \{\mathbf{z} : \cup_i h_{i,S,m}(\mathbf{z};\mathbf{r}) < 0\}$ or $\{\mathbf{z} : \cap_i h_{i,S,m}(\mathbf{z};\mathbf{r}) < 0\}$ be a failure set, as a result of the S-variate, the mth-order DD-GPCE $h_{S,m}(\mathbf{Z};\mathbf{r})$ of $h(\mathbf{Z};\mathbf{r})$ or $h_{i,S,m}(\mathbf{Z};\mathbf{r})$ of $h_i(\mathbf{Z};\mathbf{r})$. Then, the DD-GPCE estimate of the failure probability is

$$\begin{aligned} \mathbb{P}_{\mathbf{g}}\big[\mathbf{Z} \in \bar{\Omega}_{F,S,m}\big] &:= \int_{\bar{\mathbb{A}}^N} I_{\bar{\Omega}_{F,S,m}}(\mathbf{z};\mathbf{r}) f_{\mathbf{Z}}(\mathbf{z};\mathbf{g}) d\mathbf{z} \\ &:= \mathbb{E}_{\mathbf{g}}\Big[I_{\bar{\Omega}_{F,S,m}}(\mathbf{Z};\mathbf{r})\Big] \\ &= \lim_{\bar{L}\to\infty} \frac{1}{\bar{L}} \sum_{l=1}^{\bar{L}} I_{\bar{\Omega}_{F,S,m}}(\mathbf{z}^{(l)};\mathbf{r}), \end{aligned} \tag{31}$$

where $\mathbf{z}^{(l)}$ is the lth realization of $\mathbf{Z}$, $\bar{L}$ is the sample size, and $I_{\bar{\Omega}_{F,S,m}}$ is another indicator function such that

$$I_{\bar{\Omega}_{F,S,m}} = \begin{cases} 1, & \mathbf{z} \in \bar{\Omega}_{F,S,m}, \\ 0, & \mathbf{z} \notin \bar{\Omega}_{F,S,m}. \end{cases} \tag{32}$$

Note that the MCS of DD-GPCE approximation in Eq. (31) should not be confused with crude MCS commonly used for producing benchmark results. The crude MCS, which requires numerical calculations of h or h_i for input samples $\mathbf{z}^{(l)}$, $l = 1, \ldots, L$, can be expensive or even prohibitive, particularly when the sample size $\bar{L}$ needs to be very large for estimating small failure probabilities. In contrast, the MCS embedded in the DD-GPCE approximation requires evaluations of simple polynomial functions that describe $h_{S,m}$ or $h_{i,S,m}$. Therefore, an arbitrarily large sample size can be accommodated in the DD-GPCE approximation.

The DD-GPCE presented here can be viewed as a reconfigured GPCE, where the basis set of multivariate orthonormal polynomials of regular GPCE has been reshuffled and pruned according to the chosen degree of interaction and expansion order. However, DD-GPCE is not the same as the generalized polynomial dimensional decomposition (GPDD) [35,48], where the basis set of multivariate orthogonal polynomials is also developed dimensionwise and hierarchically but satisfying a few distinguishing properties of the generalized analysis-of-variance dimensional decomposition [49]. A meticulous comparison between DD-GPCE and GPDD is beyond the scope of this current work.

4. DESIGN SENSITIVITY ANALYSIS

When solving RDO or RBDO problems with a gradient-based optimization algorithm, such as sequential linear or quadratic programming, at least the first-order derivatives of the first two moments or the failure probability of $h_l(\mathbf{Z};\mathbf{r})$, $l = 0, 1, \ldots, K$, with respect to each design variable d_k, $k = 1, \ldots, M$, are demanded. In this section, an analytical design sensitivity formulation, coupling the DD-GPCE approximation and score functions for dependent input random variables, is presented. For such sensitivity analysis, the following regularity conditions are necessary:

1. The PDF $f_{\mathbf{Z}}(\mathbf{z};\mathbf{g})$ of $\mathbf{Z}$ is continuous. Also, the partial derivative $\partial f_{\mathbf{Z}}(\mathbf{z};\mathbf{g})/\partial g_k$, $k = 1, \ldots, M$, exists and is finite for all possible values of $\mathbf{z}$ and g_k. Moreover, the failure probability associated with the performance function $h(\mathbf{Z};\mathbf{r})$ is a differentiable function of $\mathbf{g}$.

2. There exists a Lebesgue integrable dominating function $t(\mathbf{z})$ such that, for $r = 1, 2$ and $k = 1, \ldots, M$,

$$\left| h^r(\mathbf{z};\mathbf{r}) \frac{\partial f_{\mathbf{Z}}(\mathbf{z};\mathbf{g})}{\partial d_k} \right| \leq t(\mathbf{z}), \tag{33}$$

and

$$\left| I_{\bar{\Omega}_F}(\mathbf{z};\mathbf{r}) \frac{\partial f_{\mathbf{Z}}(\mathbf{z};\mathbf{g})}{\partial d_k} \right| \leq t(\mathbf{z}). \tag{34}$$

Note that the sensitivity formulation proposed in the following subsections is not limited to either independent or dependent random variables.

4.1 Score Function

Suppose the first-order derivatives of the first two moments $\mathbb{E}_{\mathbf{g}}[h^r(\mathbf{Z};\mathbf{r})]$, $r = 1, 2$, and the failure probability $\mathbb{P}_{\mathbf{g}}\left[\mathbf{Z} \in \bar{\Omega}_F\right]$ corresponding to a generic performance function $h(\mathbf{Z};\mathbf{r})$ with respect to design variables d_k, $k = 1, \ldots, M$, have to be computed in solving the RDO in Eq. (12) and RBDO in Eq. (15) by a gradient-based design optimization algorithm. Let

$$\mathbb{E}_{\mathbf{g}}[g(\mathbf{Z};\mathbf{r})] := \int_{\bar{\mathbb{A}}^N} g(\mathbf{z};\mathbf{r}) f_{\mathbf{Z}}(\mathbf{z};\mathbf{g}) d\mathbf{z} \tag{35}$$

be a generic probabilistic response, where $g(\mathbf{z};\mathbf{r})$ is either $h^r(\mathbf{z};\mathbf{r})$, $r = 1, 2$, for statistical moment analysis or $I_{\bar{\Omega}_F}(\mathbf{z};\mathbf{r})$ for reliability analysis. Then, applying the partial derivative with respect to d_k to $\mathbb{E}_{\mathbf{g}}[g(\mathbf{Z};\mathbf{r})]$ and invoking the chain rule and the Lebesgue dominated convergence theorem [50], which allows one to interchange the differential and integral operators, produces the first-order sensitivities

$$\begin{aligned} \frac{\partial \mathbb{E}_{\mathbf{g}}[g(\mathbf{Z};\mathbf{r})]}{\partial d_k} &= \frac{\partial}{\partial d_k} \int_{\bar{\mathbb{A}}^N} g(\mathbf{z};\mathbf{r}) f_{\mathbf{Z}}(\mathbf{z};\mathbf{g}) d\mathbf{z} \\ &= \frac{\partial g_k}{\partial d_k} \frac{\partial}{\partial g_k} \int_{\bar{\mathbb{A}}^N} g(\mathbf{z};\mathbf{r}) f_{\mathbf{Z}}(\mathbf{z};\mathbf{g}) d\mathbf{z} \\ &= \frac{\partial g_k}{\partial d_k} \int_{\bar{\mathbb{A}}^N} g(\mathbf{z};\mathbf{r}) \frac{\partial \ln f_{\mathbf{Z}}(\mathbf{z};\mathbf{g})}{\partial g_k} f_{\mathbf{Z}}(\mathbf{z};\mathbf{g}) d\mathbf{z}, \quad k = 1, \ldots, M, \end{aligned} \tag{36}$$

where $\partial g_k/\partial d_k = 1$ or r_{i_k} for the shifting or scaling transformations, respectively. Define by

$$s_k(\mathbf{Z};\mathbf{g}) := \frac{\partial \ln f_{\mathbf{Z}}(\mathbf{Z};\mathbf{g})}{\partial g_k} \tag{37}$$

the first-order score function [51,52] for the variable g_k. Usually, the score functions can be determined numerically or analytically.

Combining Eqs. (36) and (37) results in

$$\begin{aligned}\frac{\partial \mathbb{E}_{\mathbf{g}}[g(\mathbf{Z};\mathbf{r})]}{\partial d_k} &= \frac{\partial g_k}{\partial d_k}\int_{\bar{\mathbb{A}}^N} g(\mathbf{z};\mathbf{r}) s_k(\mathbf{z};\mathbf{g}) f_{\mathbf{Z}}(\mathbf{z};\mathbf{g}) d\mathbf{z} \\ &= \frac{\partial g_k}{\partial d_k}\mathbb{E}_{\mathbf{g}}[g(\mathbf{Z};\mathbf{r}) s_k(\mathbf{Z};\mathbf{g})], \quad k = 1,\ldots,M.\end{aligned} \tag{38}$$

According to Eqs. (35) and (38), the generic probabilistic response and its sensitivities have both been formulated as expectations of stochastic quantities with respect to the same probability measure, facilitating their concurrent evaluations in a single stochastic simulation or analysis.

4.2 Sensitivity of Statistical Moments

Selecting $g(\mathbf{z};\mathbf{r})$ to be $h^r(\mathbf{z};\mathbf{r})$ and then replacing $h(\mathbf{z};\mathbf{r})$ with its S-variate mth-order DD-GPCE approximation $h_{S,m}(\mathbf{z};\mathbf{r})$ in the last line of Eq. (38), the resultant approximation of the sensitivities of the rth-order moment is obtained as

$$\frac{\partial g_k}{\partial d_k}\mathbb{E}_{\mathbf{g}}[h^r_{S,m}(\mathbf{Z};\mathbf{r}) s_k(\mathbf{Z};\mathbf{g})] = \frac{\partial g_k}{\partial d_k}\int_{\bar{\mathbb{A}}^N} h^r_{S,m}(\mathbf{z};\mathbf{r}) s_k(\mathbf{z};\mathbf{g}) f_{\mathbf{Z}}(\mathbf{z};\mathbf{g}) d\mathbf{z}. \tag{39}$$

If s_k is square-integrable, then it can be expanded with respect to the same orthornormal basis functions. For $0 \le S' \le N$ and $S' \le m' < \infty$, the result is S'-variate, m'th-order DD-GPCE

$$s_{k,S',m'}(\mathbf{Z};\mathbf{g}) = \sum_{i=2}^{L_{N,S',m'}} D_{k,i}(\mathbf{g})\Psi_i(\mathbf{Z};\mathbf{g}), \tag{40}$$

with its expansion coefficients

$$D_{k,i}(\mathbf{g}) = \int_{\bar{\mathbb{A}}^N} s_k(\mathbf{z};\mathbf{g})\Psi_i(\mathbf{z};\mathbf{g}) f_{\mathbf{Z}}(\mathbf{z};\mathbf{g}) d\mathbf{z},\ i = 2,\ldots,\infty,$$

and $D_{k,1}(\mathbf{g}) = 0$ [29].

Finally, setting $r = 1$ and $r = 2$ in Eq. (39) yields the approximate sensitivity of the first and second moments as follows:

$$\frac{\partial \mathbb{E}_{\mathbf{g}}[h_{S,m}(\mathbf{Z};\mathbf{r})]}{\partial d_k} = \frac{\partial g_k}{\partial d_k}\sum_{i=2}^{L_{\min}} C_i(\mathbf{r}) D_{k,i}(\mathbf{g}) \tag{41}$$

and

$$\frac{\partial \mathbb{E}_{\mathbf{g}}[h^2_{S,m}(\mathbf{Z};\mathbf{r})]}{\partial d_k} = \frac{\partial g_k}{\partial d_k}\sum_{i_1=1}^{L_{N,S,m}}\sum_{i_2=1}^{L_{N,S,m}}\sum_{i_3=2}^{L_{N,S',m'}} C_{i_1}(\mathbf{r})C_{i_2}(\mathbf{r})D_{k,i_3}(\mathbf{g})\mathbb{E}_{\mathbf{g}}\left[\prod_{p=1}^{3}\Psi_{i_p}(\mathbf{Z};\mathbf{g})\right], \tag{42}$$

respectively, where $L_{\min} := \min(L_{N,S,m}, L_{N,S',m'})$. The approximate sensitivities in Eqs. (41) and (42) converge to $\partial \mathbb{E}_{\mathbf{g}}[h(\mathbf{Z};\mathbf{r})] \,/\, \partial d_k$ and $\partial \mathbb{E}_{\mathbf{g}}[h^2(\mathbf{Z};\mathbf{r})] \,/\, \partial d_k$, respectively, when $S = N$, $S' = N$, $m \to \infty$, and $m' \to \infty$.

In Eq. (42), the expectations of products of three distinct multivariate orthonormal polynomials need to be calculated $L_{N,S,m} \times L_{N,S,m} \times L_{N,S',m'}$ times. For an arbitrary dependent random vector Z, such expectations or integrals cannot be calculated exactly. This is in contrast to independent variables where exact solutions exist for a few classical distributions [53,54]. Therefore, for dependent variables, they must be estimated, say, by numerical integration or sampling methods. If the dimension is too high, then the sampling methods, such as MCS, QMCS, or Latin hypercube sampling, can be used to estimate these integrals [29].

4.3 Sensitivity of Failure Probability

Selecting $g(\mathbf{z};\mathbf{r})$ to be $I_{\Omega_F}(\mathbf{z};\mathbf{r})$ and then replacing $h(\mathbf{z};\mathbf{r})$ with its S-variate, mth-order DD-GPCE approximation $h_{S,m}(\mathbf{z};\mathbf{r})$ in the second line of Eq. (38), the resultant approximation of the sensitivities of the failure probability is obtained as

$$\frac{\partial g_k}{\partial d_k}\mathbb{E}_{\mathbf{g}}\Big[I_{\bar{\Omega}_{F,S,m}}(\mathbf{Z};\mathbf{r})s_k(\mathbf{Z};\mathbf{g})\Big] = \frac{\partial g_k}{\partial d_k}\lim_{\bar{L}\to\infty}\frac{1}{\bar{L}}\sum_{l=1}^{\bar{L}}\Big[I_{\bar{\Omega}_{F,S,m}}(\mathbf{z}^{(l)})s_k(\mathbf{z}^{(l)};\mathbf{g})\Big], \tag{43}$$

where $\bar{L}$ is the sample size and $\mathbf{z}^{(l)}$ is the lth realization of $\mathbf{Z}$. Again, the sensitivity in Eq. (43) is easily and inexpensively determined by sampling elementary polynomial functions that describe $h_{S,m}$ and known score function s_k.

It is important to clarify that the approximate sensitivities in Eqs. (41)–(43) are obtained not by taking partial derivatives of the approximate first two moments and failure probability in Eqs. (29)–(31), respectively, with respect to g_k. Instead, it results from replacing h with $h_{S,m}$ in the expectation describing Eqs. (39) and (43).

The incorporation of score functions has the desirable property that it requires differentiating only the underlying PDF $f_{\mathbf{Z}}(\mathbf{z};\mathbf{g})$. The resulting score functions can be easily and, in most cases, analytically determined. If the performance function is not differentiable or discontinuous—for example, the indicator function that comes from reliability analysis—the proposed method still allows evaluation of the sensitivity if the density function is differentiable. In reality, the density function is often smoother than the performance function, and therefore the proposed sensitivity methods are able to calculate sensitivities for a wide variety of complex mechanical systems.

5. PROPOSED METHOD FOR STOCHASTIC DESIGN OPTIMIZATION

The DD-GPCE approximations, described in the preceding sections, are intended to evaluate the objective and/or constraint functions $c_l(\mathbf{d})$, $l = 0,\ldots,K$, and their design sensitivities from a single stochastic analysis. For the RBDO problem in Eq. (15), its objective function is a simple and explicit deterministic mapping between design variables and output, thus not demanding such a stochastic analysis. However, it is conceivable that the objective function may also be defined as the first two moments of a response function of random variables whose distribution parameters are specified by design variables, yielding reliability-based robust design optimization. For instance, let $h_0(\mathbf{z};\mathbf{r}) \in L^2(\Omega_{\mathbf{d}},\mathcal{F}_{\mathbf{d}},\mathbb{P}_{\mathbf{d}})$ be a random output function of an input random vector $\mathbf{z} := (z_1,\ldots,z_N)^\intercal$ with known PDF $f_{\mathbf{Z}}(\mathbf{z};\mathbf{g})$. Then, the objective function in Eq. (15) can be

$$c_0(\mathbf{d}) := w_1\frac{\mathbb{E}_{\mathbf{d}(\mathbf{g})}[h_0(\mathbf{Z};\mathbf{r})]}{\mu_0^*} + w_2\frac{\sqrt{\mathrm{var}_{\mathbf{d}(\mathbf{g})}[h_0(\mathbf{Z};\mathbf{r})]}}{\sigma_0^*},$$

where $\mathbb{E}_{\mathbf{g}(\mathbf{d})}[h_0(\mathbf{Z};\mathbf{r})] := \int_{\bar{\mathbb{A}}^N} h_0(\mathbf{z};\mathbf{r})f_{\mathbf{Z}}(\mathbf{z};\mathbf{g}(\mathbf{d}))d\mathbf{z}$; $\mathrm{var}_{\mathbf{g}(\mathbf{d})}[h_l(\mathbf{Z};\mathbf{r})] := \mathbb{E}_{\mathbf{g}(\mathbf{d})}\big[h_l(\mathbf{Z};\mathbf{r}) - \mathbb{E}_{\mathbf{g}(\mathbf{d})}[h_l(\mathbf{Z};\mathbf{r})]\big]^2$; $w_1 \in \mathbb{R}_0^+$ and $w_2 \in \mathbb{R}_0^+$ are two non-negative, real-valued weights such that $w_1 + w_2 = 1$; and $\mu_0^* \in \mathbb{R}\setminus\{0\}$ and $\sigma_0^* \in \mathbb{R}_0^+\setminus\{0\}$ are two non-zero, real-valued scaling factors.

A straightforward integration of stochastic analyses, design sensitivity analysis, and an appropriate optimization algorithm is expected to yield a convergent solution of the RDO and RBDO problems in Eqs. (12) and (15), respectively. However, new stochastic analyses and design sensitivity analysis by recomputing the DD-GPCE coefficients are demanded at every design iteration, thus easily becoming computationally intensive. To reduce such computational costs, the single-step and multipoint single-step processes will be introduced in the following subsections, which were studied to be employed with the regular GPCE in the authors' prequels [9,29].

5.1 Single-Step DD-GPCE

The single-step DD-GPCE is intended to solve all of the RDO and RBDO problems in Eqs. (12) and (15) from a single stochastic analysis by circumventing the demand to recalculate the DD-GPCE coefficients from a new input-output data set in every design iteration. However, it is predicated on two important assumptions: (1) an S-variate,

mth-order DD-GPCE approximation $h_{S,m}(\mathbf{Z};\mathbf{r})$ of $h(\mathbf{Z};\mathbf{r})$ at the initial design is adequate for all possible designs; and (2) the DD-GPCE coefficients for a new design, determined by recycling those for an old design, are acceptable for their accuracy.

Under these two assumptions, let vectors $\mathbf{r}$ and $\mathbf{r}'$ represent the old and new designs, respectively. Assume that DD-GPCE coefficients $C_i(\mathbf{r})$, $i = 1,\ldots,L_{N,S,m}$, for the old design $\mathbf{r}$ have been already estimated from the old input-output data $\{\mathbf{z}^{(l)}, h(\mathbf{z}^{(l)};\mathbf{r})\}_{l=1}^{L}$. Then, DD-GPCE coefficients $C_i(\mathbf{r}')$, $i = 1,\ldots,L_{N,S,m}$, for the new design $\mathbf{r}'$ are determined by adjusting the input data set $\{\mathbf{z}^{(l)}\}_{l=1}^{L}$ to the following one $\{\mathbf{z}'^{(l)}\}_{l=1}^{L}$, as

$$\mathbf{z}'^{(l)} = \begin{cases} \mathbf{z}^{(l)} - \mathbf{r}' + \mathbf{r}, & \text{in shifting,} \\ \operatorname{diag}\left(\dfrac{r_1}{r'_1},\ldots,\dfrac{r_N}{r'_N}\right)\mathbf{z}^{(l)}, & \text{in scaling.} \end{cases} \tag{44}$$

In the shifting case of Eq. (44), the new output value at the lth input sample is

$$\begin{aligned} h(\mathbf{z}^{(l)};\mathbf{r}') &:= y(\mathbf{z}^{(l)} - \mathbf{r}') = y(\mathbf{z}^{(l)} - \mathbf{r}' + \mathbf{r} - \mathbf{r}) \\ &= y(\mathbf{z}'^{(l)} - \mathbf{r}) =: h(\mathbf{z}'^{(l)};\mathbf{r}), \end{aligned} \tag{45}$$

where $\mathbf{z}'^{(l)} := \mathbf{z}^{(l)} - \mathbf{r}' + \mathbf{r}$ is the adjusted lth input sample. In the scaling case of (44), the new output value at the lth input sample is

$$\begin{aligned} h(\mathbf{z}^{(l)};\mathbf{r}') &:= y\left(\operatorname{diag}\left[\frac{1}{r'_1},\ldots,\frac{1}{r'_N}\right]\mathbf{z}^{(l)}\right) \\ &= y\left(\operatorname{diag}\left[\frac{1}{r_1},\ldots,\frac{1}{r_N}\right]\operatorname{diag}\left[\frac{r_1}{r'_1},\ldots,\frac{r_N}{r'_N}\right]\mathbf{z}^{(l)}\right) \\ &= y\left(\operatorname{diag}\left[\frac{1}{r_1},\ldots,\frac{1}{r_N}\right]\mathbf{z}'^{(l)}\right) =: h(\mathbf{z}'^{(l)};\mathbf{r}), \end{aligned} \tag{46}$$

where $\mathbf{z}'^{(l)} := \operatorname{diag}[r_1/r'_1,\ldots,r_N/r'_N]\mathbf{z}^{(l)}$ is the adjusted lth input sample. These adjustments are meant to construct an input-output data set for new designs from DD-GPCE coefficients $C_i(\mathbf{r})$ for the old design, that is,

$$h(\mathbf{z}^{(l)};\mathbf{r}') = h(\mathbf{z}'^{(l)};\mathbf{r}) \approx \sum_{i=1}^{L_{N,S,m}} C_i(\mathbf{r})\Psi_i(\mathbf{z}'^{(l)};\mathbf{g}), \tag{47}$$

where the last term indicates the S-variate, mth-order DD-GPCE approximation. Applying Eq. (47) to Eq. (B.3) yields an estimate of the mean square residual,

$$\hat{e}''_{S,m} := \frac{1}{L}\sum_{l=1}^{L}\left[\sum_{i=1}^{L_{N,S,m}} C_i(\mathbf{r})\Psi_i(\mathbf{z}'^{(l)};\mathbf{g}) - \sum_{i=1}^{L_{N,S,m}} C_i(\mathbf{r}')\Psi_i(\mathbf{z}^{(l)};\mathbf{g})\right]^2, \tag{48}$$

the minimization of which by SLS produces the best estimates of DD-GPCE coefficients for the new design. Compared with the minimization of $\hat{e}_{S,m}$ in Eq. (B.3), the calculation of new output data using the original performance function $h(\mathbf{z}^{(l)};\mathbf{r}')$ is not demanded. Instead, the new output data are estimated by recycling the old coefficients and calculating basis function values at the adjusted input data $\mathbf{z}'$, as shown in Eq. (44). Subsequently, new stochastic analyses and design sensitivity analysis, both employing S-variate, mth-order DD-GPCE approximations from the initial design, are performed with little extra cost during all design iterations. Therefore, the single-step process holds the potential to substantially reduce the computational effort in solving RDO and RBDO problems.

5.2 Multipoint Single-Step DD-GPCE

The single-step process, described in the foregoing section, is predicated on accurate DD-GPCE approximations of stochastic responses, supplying surrogates of objective and/or constraint functions for the entire design space.

Therefore, if the truncation parameters S and m of DD-GPCE are demanded to be exceedingly large to capture a high-dimensional nonlinear stochastic response, this global method may lead to a computationally taxing design process. In such a case, employing DD-GPCE of only a low-variate, low-order approximation may be inappropriate, failing to find a true optimal solution. An appealing substitute, referred to as the multipoint single-step DD-GPCE (MPSS-DD-GPCE) method, asks for local implementations of the DD-GPCE approximation that are built on subregions of the entire design space. According to this latter method, the original RDO or RBDO problem is swapped for a series of local RDO or RBDO problems, respectively, where the objective and/or constraint functions in each local RDO or RBDO problem represent their multipoint approximations [37]. The design solution of an individual local RDO or RBDO problem, obtained by the single-step DD-GPCE method, constitutes the initial design for the next local RDO or RBDO problem. Then, the move limits are updated, and the optimization is repeated iteratively until the optimal solution is acquired. Due to the local approach, the MPSS-DD-GPCE method is expected to solve practical engineering problems using low-degree DD-GPCE approximations.

For the rectangular design space

$$\mathcal{D} = \bigtimes_{k=1}^{k=M} [d_{k,L}, d_{k,U}] \subseteq \mathbb{R}^M \tag{49}$$

of the RDO and RBDO problems described in Eqs. (12) and (15), denote by $q' = 1, 2, \ldots, Q' \in \mathbb{N}$ an index indicating the q'th subregion of $\mathcal{D}$ with the initial design vector $\mathbf{d}_0^{(q')} = (d_{1,0}^{(q')}, \ldots, d_{M,0}^{(q')})^\intercal$. Given a sizing factor $0 < \beta_k^{(q')} \leq 1$, the domain of the q'th subregion is expressed by

$$\mathcal{D}^{(q')} = \bigtimes_{k=1}^{k=M} \left[d_{k,0}^{(q')} - \beta_k^{(q')} \frac{(d_{k,U} - d_{k,L})}{2},\ d_{k,0}^{(q')} + \beta_k^{(q')} \frac{(d_{k,U} - d_{k,L})}{2} \right] \subseteq \mathcal{D} \subseteq \mathbb{R}^M, \quad q' = 1, \ldots, Q'. \tag{50}$$

According to the multipoint design process, the RDO and RBDO problems in Eqs. (12) and (15) are transformed to a succession of local RDO and RBDO problems for Q' subregions as follows.

- Local RDO problem.

  For the q'th subregion, the local RDO problem requires one to solve

$$\begin{aligned} \min_{\mathbf{d} \in \mathcal{D}^{(q')} \subseteq \mathbb{R}^M} \ & \tilde{c}_{0,S,m}^{(q')}(\mathbf{d}) := G\left(\mathbb{E}_{\mathbf{g}}[\tilde{h}_{0,S,m}^{(q')}(\mathbf{Z};\mathbf{r})], \sqrt{\mathrm{var}_{\mathbf{g}}[\tilde{h}_{0,S,m}^{(q')}(\mathbf{Z};\mathbf{r})]} \right), \\ \text{subject to } \ & \tilde{c}_{l,S,m}^{(q')}(\mathbf{d}) := \alpha_l \sqrt{\mathrm{var}_{\mathbf{g}}[\tilde{h}_{l,S,m}^{(q')}(\mathbf{Z};\mathbf{r})]} - \mathbb{E}_{\mathbf{g}}[\tilde{h}_{l,S,m}^{(q')}(\mathbf{Z};\mathbf{r})] \leq 0, \\ & d_k \in \left[d_{k,0}^{(q')} - \beta_k^{(q')}(d_{k,U} - d_{k,L}) \,/\, 2,\ d_{k,0}^{(q')} + \beta_k^{(q')}(d_{k,U} - d_{k,L}) \,/\, 2 \right], \\ & l = 1, \ldots, K, \quad k = 1, \ldots, M, \end{aligned} \tag{51}$$

  where

$$\mathbb{E}_{\mathbf{g}}\left[\tilde{h}_{l,S,m}^{(q')}(\mathbf{Z};\mathbf{r})\right] := \int_{\bar{\mathbb{A}}^N} \tilde{h}_{l,S,m}^{(q')}(\mathbf{z};\mathbf{r}) f_{\mathbf{Z}}\big(\mathbf{z}; \mathbf{g}(\mathbf{d})\big) d\mathbf{z}, \tag{52}$$

$$\mathrm{var}_{\mathbf{g}}\left[\tilde{h}_{l,S,m}^{(q')}(\mathbf{Z};\mathbf{r})\right] := \mathbb{E}_{\mathbf{g}}\left[\tilde{h}_{l,S,m}^{(q')}(\mathbf{Z};\mathbf{r}) - \mathbb{E}_{\mathbf{g}}[\tilde{h}_{l,S,m}^{(q')}(\mathbf{Z};\mathbf{r})]\right]^2, \tag{53}$$

  and $\tilde{c}_{l,S,m}^{(q')}(\mathbf{d})$ and $\tilde{h}_{l,S,m}^{(q')}(\mathbf{Z};\mathbf{r})$, $l = 0, 1, \ldots, K$, are the S-variate, mth-order DD-GPCE approximations of $c_l(\mathbf{d})$ and $h_l(\mathbf{Z};\mathbf{r})$, respectively, for the q'th subregion. Also, $d_{k,0}^{(q')} - \beta_k^{(q')}(d_{k,U} - d_{k,L})/2$ and $d_{k,0}^{(q')} + \beta_k^{(q')}(d_{k,U} - d_{k,L})/2$, known as the move limits, are the lower and upper bounds, respectively, of the subregion $\mathcal{D}^{(q')}$.

- Local RBDO problem.

  For the q'th subregion, the local RBDO problem requires one to solve

$$\begin{aligned}
&\min_{\mathbf{d}\in\mathcal{D}^{(q')}\subseteq\mathbb{R}^M} \quad \tilde{c}^{(q')}_{0,S,m}(\mathbf{d}) \\
&\text{subject to} \quad \tilde{c}^{(q')}_{l,S,m}(\mathbf{d}) := \mathbb{P}_{\mathbf{g}}[\mathbf{Z}\in\tilde{\bar{\Omega}}^{(q')}_{F,l,S,m}(\mathbf{d})] - p_l \le 0, \\
&\qquad\qquad d_k \in \left[d^{(q')}_{k,0} - \beta^{(q')}_k (d_{k,U}-d_{k,L})\,/\,2,\ d^{(q')}_{k,0} + \beta^{(q')}_k (d_{k,U}-d_{k,L})\,/\,2\right], \\
&\qquad\qquad l=1,\dots,K;\ \ k=1,\dots,M,
\end{aligned} \tag{54}$$

where $\tilde{c}^{(q')}_{0,S,m}$, $\tilde{\bar{\Omega}}^{(q')}_{F,l,S,m}(\mathbf{d})$, and $\tilde{c}^{(q')}_{l,S,m}(\mathbf{d})$, $l=1,\dots,K$, are the S-variate, mth-order DD-GPCE approximations of $c_0(\mathbf{d})$, $\bar{\Omega}_{F,l}(\mathbf{d})$, and $c_l(\mathbf{d})$, respectively, for the q'th subregion problem, and $\tilde{\bar{\Omega}}^{(q')}_{F,l,S,m}(\mathbf{d})$ is defined using the S-variate, mth-order DD-GPCE approximation $\tilde{h}^{(q')}_{l,S,m}(\mathbf{z};\mathbf{r})$ of $h_l(\mathbf{z})$, and $d^{(q')}_{k,0} - \beta^{(q')}_k (d_{k,U}-d_{k,L})/2$ and $d^{(q')}_{k,0} + \beta^{(q')}_k (d_{k,U}-d_{k,L})\,/\,2$, known as the move limits, are the lower and upper bounds, respectively, of the subregion $\mathcal{D}^{(q')}$.

The multipoint single-step process is schematically depicted in Fig. 1. Here, $\mathbf{d}^{(q')}_*$ is the optimal design solution obtained using the single-step process for the q'th local RDO and RBDO problems in Eqs. (51) and (54). Setting the initial design $\mathbf{d}^{(q'+1)}_0$ to $\mathbf{d}^{(q')}_*$ for the next local RDO and RBDO problems on $\mathcal{D}^{(q'+1)}$, the process is repeated until a final, convergent solution $\mathbf{d}^*$ that satisfies all constraint conditions is attained. The flow chart of the method, referred to as MPSS-DD-GPCE, is presented in Figs. 2 and 3 with supplementary explanations of each step of the method, as follows.

Step 1. Set termination criteria $0 < \epsilon_1, \epsilon_2 \ll 1$; set tolerances for sizing subregions $0 < \epsilon_3, \epsilon_4, \epsilon_5, \epsilon_6, \epsilon_7 < 1$; initialize size parameters $0 < \beta^{(q')}_k \le 1$, $k=1,\dots,M$, of $\mathcal{D}^{(q')}$; and set an initial design vector $\mathbf{d}^{(q')}_0 = (d^{(q')}_{1,0},\dots,d^{(q')}_{M,0})$. The initial design can be in either feasible or infeasible domains with respect to the constraints.

Step 2. Transform the input random vector $\mathbf{X}$ to a new random vector $\mathbf{Z}$ such that $\mathbb{E}_{\mathbf{d}}[Z_{i_k}] = g_k = 0$ or 1, $k=1,\dots,M$, by shifting or scaling, respectively, described in Section 2.2.

Step 3. Select $0 \le S \le N$ and $S \le m < \infty$ of DD-GPCE approximations for performance functions $h_l(\mathbf{z};\mathbf{r})$, $l=0,1,\dots,K$. Construct an $L_{N,S,m}$-dimensional vector of measure consistent orthonormal polynomials $\mathbf{\Psi}_{S,m}(\mathbf{Z};\mathbf{g})$ through the three-step algorithm, described in Section 3.2.

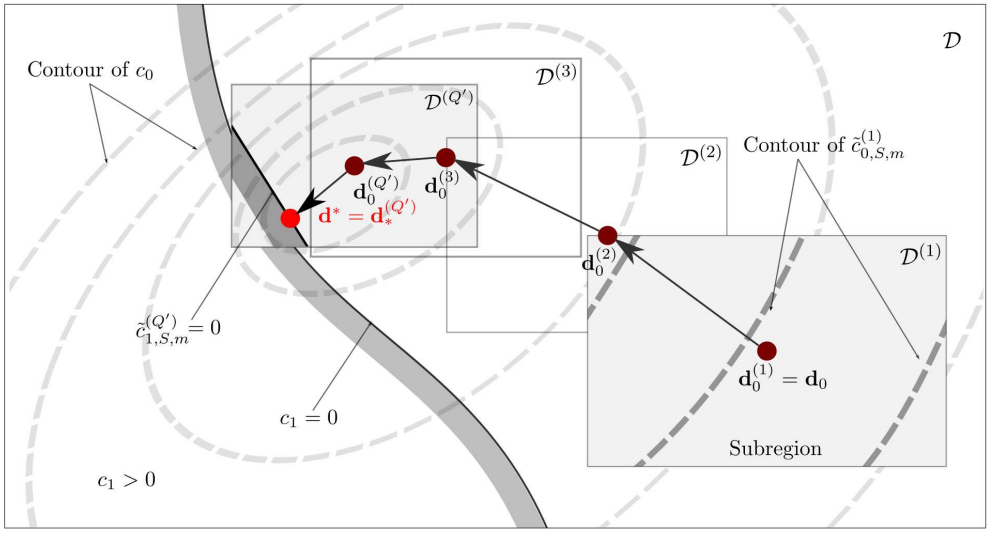

FIG. 1: A schematic description of the multipoint single-step design process during Q' iterations to get the final optimum $\mathbf{d}^*$

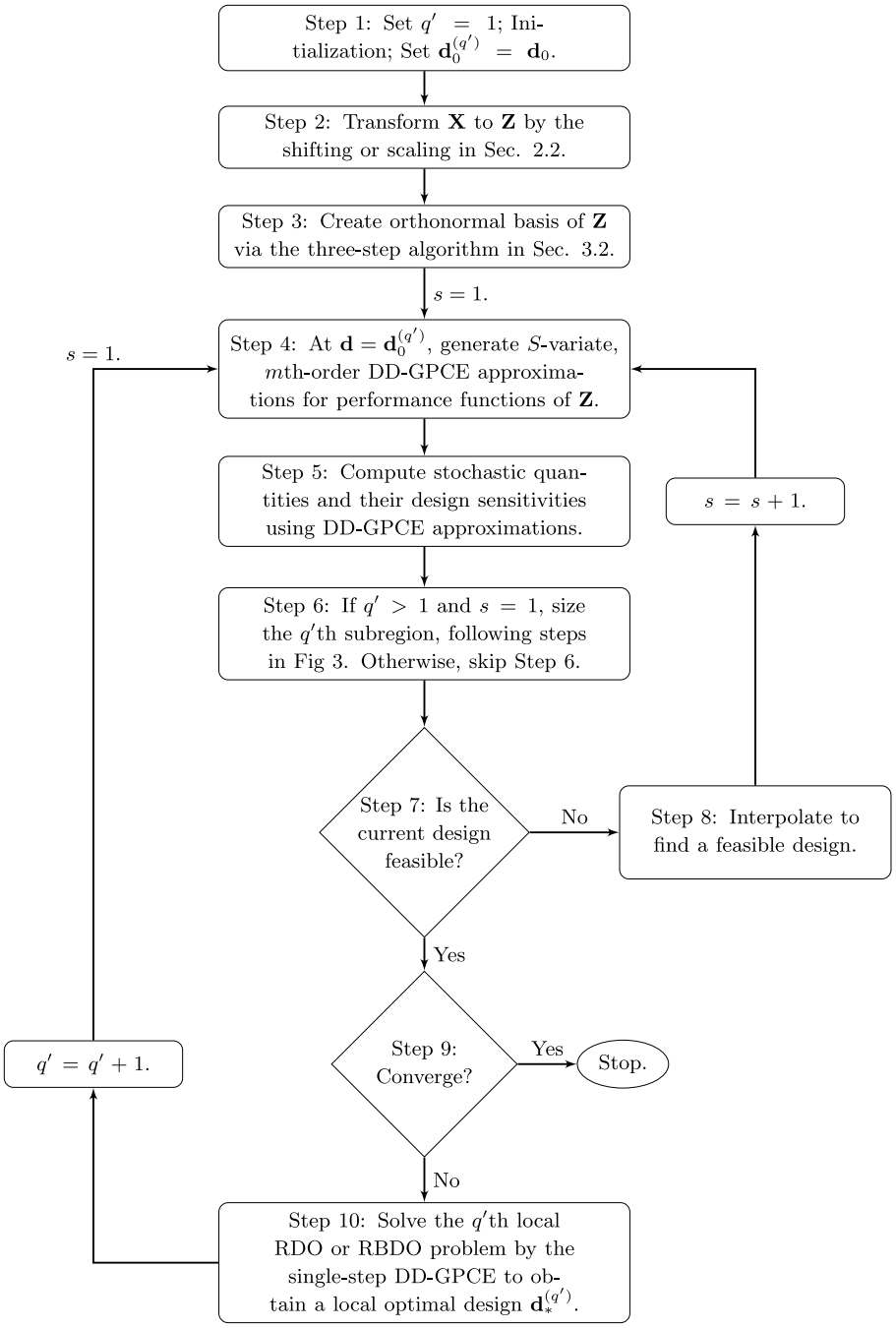

FIG. 2: A flow chart of the MPSS-DD-GPCE method

Step 4. Update the current design vector $\mathbf{d}$, as follows. If $q' = 1$, create input samples $\{\mathbf{z}^{(l)}\}_{l=1}^{l=L}$ and $\{\mathbf{z}^{(l)}\}_{l=1}^{l=\bar{L}}$, where usually $\bar{L} \gg L$, via the MCS or other experimental design method. Use the input samples to construct an input-output data set $\{\mathbf{z}^{(l)}, h(\mathbf{z}^{(l)}; \mathbf{r})\}_{l=1}^{L}$ of sample size $L > L_{N,S,m}$ (say, $L/L_{N,S,m} \geq 3$). If $q' > 1$, reuse the input samples to generate new input-output data sets $\{\mathbf{z}^{(l)}, h(\mathbf{z}^{(l)}; \mathbf{r}')\}_{l=1}^{L}$. In every q' step, use SLS to estimate DD-GPCE coefficients with respect to $\mathbf{\Psi}_{S,m}(\mathbf{z}; \mathbf{g})$ using the new input-output data set.

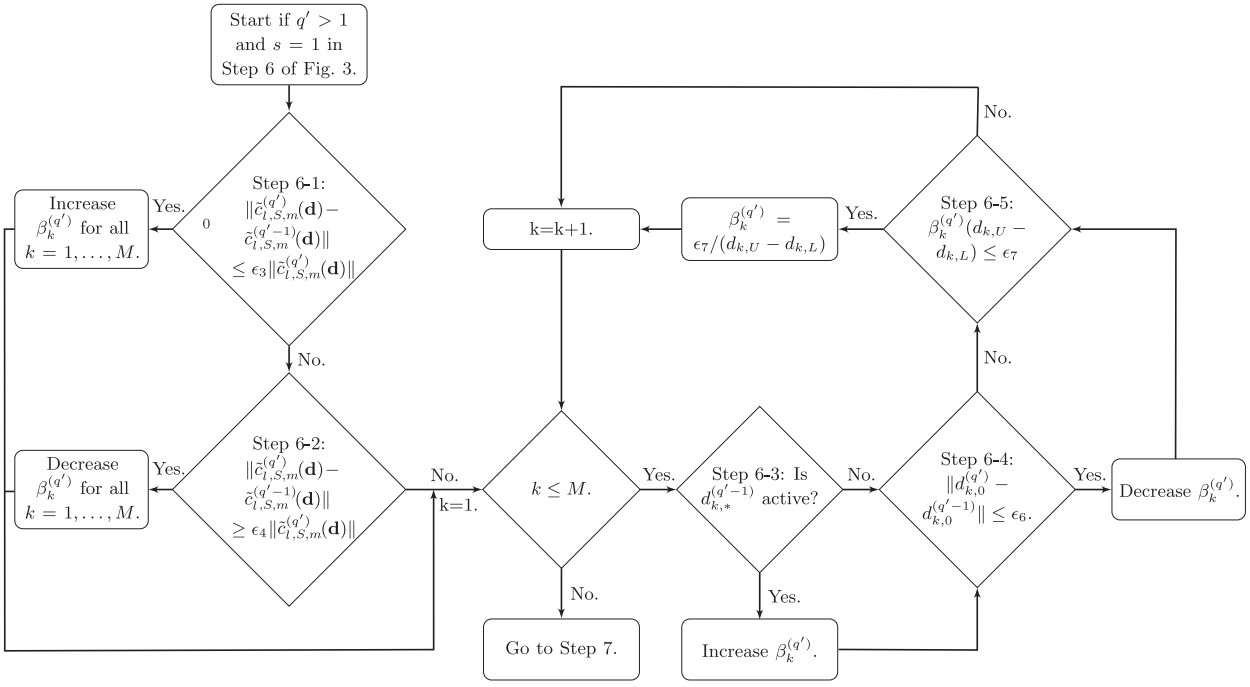

FIG. 3: A flow chart of sizing the q'th subregion in the multipoint single-step design process

Step 5. In each iteration, conduct stochastic analyses and compute the sensitivity of the stochastic quantities with respect to design variables d_k, $k = 1, \ldots, M$, both using S-variate, mth-order DD-GPCE approximations. For the design sensitivity analysis, if $q' = 1$, construct an input-output data sets for score functions, $\{\mathbf{z}^{(l)}, s_k(\mathbf{z}^{(l)}; \mathbf{g})\}_{l=1}^{L}$ and $\{\mathbf{z}^{(l)}, s_k(\mathbf{z}^{(l)}; \mathbf{g})\}_{l=1}^{L}$, $k = 1, \ldots, M$, for statistical moment analysis and reliability analysis, respectively. Otherwise, reuse the input-output data sets of $q' = 1$. Finally, obtain the objective and constraint function values and their gradients at $\mathbf{d} = \mathbf{d}_0^{(q')}$.

Step 6. If $q' = 1$ and $s = 1$, use the initial or default values of size parameters $0 < \beta_k^{(q')} \le 1,\ k = 1, \ldots, M$, in Step 1. If $q' > 1$ and $s = 1$, modify the size parameters according to three criteria: (1) the accuracy of DD-GPCE approximations, (2) the active/inactive condition of subregion boundaries, and (3) the converging condition of current designs. Otherwise, skip Step 6. The details of the three conditions mentioned earlier are explained in the following steps.

Step 6-1. First condition: For any of $l = 0, \ldots, K$, if $||\tilde{c}^{(q')}_{l,S,m}(\mathbf{d}_0^{(q')}) - \tilde{c}^{(q'-1)}_{l,S,m}(\mathbf{d}_0^{(q')})|| \le \epsilon_3 ||\tilde{c}^{(q')}_{l,S,m}(\mathbf{d}_0^{(q')})||$, increase $\beta_k^{(q')}$ for all $k = 1, \ldots, M$. Otherwise, go to Step 6-2. One may need to control the enlargement rate, depending on the problems at hand. For instance, set $\beta_k^{(q')} = (2 - 1/\phi)\beta_k^{(q'-1)}$, where the golden ratio $\phi \approx 1.618$.

Step 6-2. First condition: For any $l = 0, \ldots, K$, if $||\tilde{c}^{(q')}_{l,S,m}(\mathbf{d}_0^{(q')}) - \tilde{c}^{(q'-1)}_{l,S,m}(\mathbf{d}_0^{(q')})|| \ge \epsilon_4 ||\tilde{c}^{(q')}_{l,S,m}(\mathbf{d}_0^{(q')})||$, decrease $\beta_k^{(q')}$ for all $k = 1, \ldots, M$. As an instance of the decrement rate, set $\beta_k^{(q')} = \beta_k^{(q'-1)}/\phi$, where the golden ratio $\phi \approx 1.618$. Otherwise, go to Step 6-3.

Step 6-3. Second condition: If $||d^{(q')}_{k,0} - d^{(q'-1)}_{k,L}|| \le \epsilon_5$ or $||d^{(q')}_{k,0} - d^{(q'-1)}_{k,U}|| \le \epsilon_5$, increase $\beta_k^{(q')}$, $k = 1, \ldots, M$. As an instance of the enlargement rate, set $\beta_k^{(q')} = (2 - 1/\phi)\beta_k^{(q'-1)}$, where the golden ratio $\phi \approx 1.618$. Otherwise, go to Step 6-4.

Step 6-4. Third condition: If $||d_{k,0}^{(q')} - d_{k,0}^{(q'-1)}|| \leq \epsilon_6$, decrease $\beta_k^{(q')}$, $k = 1, \ldots, M$. As an instance of the decrement rate, set $\beta_k^{(q')} = \beta_k^{(q'-1)}/\phi$, where the golden ratio $\phi \approx 1.618$. Otherwise, go to Step 6-5.

Step 6-5. Move limit: If $\beta_k^{(q')}(d_{k,U} - d_{k,L}) < \epsilon_7$, set $\beta_k^{(q')} = \epsilon_7/(d_{k,U} - d_{k,L})$. Otherwise, $k = k + 1$ and repeat the process until the loop condition $k \leq M$ is satisfied.

Step 7. If the current design $\mathbf{d}$ is not feasible, that is, at least one constraint condition is violated, go to Step 8. Otherwise, set $\mathbf{d}$ to the current feasible design $\mathbf{d}_f^{(q')}$, then go to Step 9.

Step 8. Interpolate between the current design $\mathbf{d}$ and the previous feasible design $\mathbf{d}_f^{(q'-1)}$. For instance, set $\mathbf{d} = \mathbf{d}_f^{(q'-1)}/\phi + (1 - 1/\phi)\mathbf{d}$, where the golden ratio $\phi \approx 1.618$. If an initial design at $q' = 1$ is infeasible, interpolate it with upper or lower bounds of the design space, or another initial guess, depending on the problems at hand.

Step 9. If any of the two termination conditions, such that (1) $\|\mathbf{d}_f^{(q')} - \mathbf{d}_f^{(q'-1)}\| \leq \epsilon_1$ and/or (2) $\|\tilde{c}_{0,S,m}^{(q')}(\mathbf{d}_f^{(q')}) - \tilde{c}_{0,S,m}^{(q')}(\mathbf{d}_f^{(q'-1)})\| \leq \epsilon_2$, are met, terminate the optimization process and set the final optimal design as $\mathbf{d}^* = \mathbf{d}_f^{(q')}$. Otherwise, go to Step 10.

Step 10. Solve the q'th local RDO or RBDO problem with the single-step process using a gradient-based algorithm, such as sequential quadratic programming, to obtain a local optimal solution $\mathbf{d}_*^{(q')}$. Then, increase the subregion count as $q' = q' + 1$. Set $\mathbf{d}_0^{(q')} = \mathbf{d}_*^{(q'-1)}$ and go to Step 4.

The multipoint single-step DD-GPCE method will be referred to as the MPSS-DD-GPCE method for the remainder of this paper.

6. NUMERICAL EXAMPLES

Three numerical examples are presented to illustrate the proposed methods for stochastic design optimization: the single-step DD-GPCE method for RDO in Example 1 and the MPSS-DD-GPCE methods in Examples 2 and 3 for RDO and RBDO, respectively. The weighted sum approach was applied to the bi-objective problem in Example 2, and single objective functions were employed in Examples 1 and 3. Readers interested in approaches other than the weighted sum should consult the authors' prior work [29]. The objective and constraint functions are either elementary mathematical functions or derived from a space truss or a more complex, industrial-scale mechanical system. Both size and shape design problems in the context of RDO and/or RBDO were solved. In all examples, the design variables are the statistical means of some or all input random variables following dependent probability distributions. Each component of the M-dimensional vector $\mathbf{g}$ is either *zero* or *one*, depending on the shifting or scaling transformations, respectively, for input random variables.

In Examples 1 and 2, the proposed DD-GPCE-based solutions are compared with those obtained by the corresponding regular GPCE-based methods. For instance, in Example 1, the regular GPCE approximation was employed in the single-step process, resulting in the single-step regular GPCE method for RDO solutions. In Example 2, the regular GPCE approximation was applied to the multipoint single-step process as well, then named the MPSS-regular-GPCE method, for comparison with the proposed MPSS-DD-GPCE method. The multivariate orthonormal polynomials consistent with the probability measure of $\mathbf{z}$ were determined using the three-step algorithms explained in Section 3.1 or 3.2 for regular GPCE or DD-GPCE approximations, respectively. The monomial moment matrix, either $\mathbf{G}_{S,m}$ in Eq. (19) or $\mathbf{G}_m$ in Eq. (A.4), was estimated by QMCS with 5×10^6 samples together with the Sobol sequence [33]. The truncation parameters $0 \leq S \leq N$ and $S \leq m < \infty$ of DD-GPCE approximations and sample sizes L and $\bar{L}$ depend on the examples and are listed in Table 1. Both DD-GPCE and regular GPCE coefficients were estimated using SLS and QMCS-generated input-output data.

As a gradient-based optimization, the sequential quadratic programming was employed to solve stochastic design optimization problems in all examples. For both the MPSS-DD-GPCE and MPSS-regular-GPCE methods, the

TABLE 1: The list of parameters (Examples 1–3): DD-GPCE and regular GPCE truncation parameters (S, m), sample sizes (L, $\bar{L}$)

Methods	S^{a}			m^{b}			L^{c}			$\bar{L}^{d}$
	y_0	y_1	s_k	y_0	y_1	s_k	y_0	y_1	s_k	
Example 1 (Case 1)										
Single-step DD-GPCE	1	1	1	8	1	1	51	9	30	—
Single-step regular GPCE	—	—	—	8	1	1	135	9	30	—
Example 1 (Case 2)										
Single-step DD-GPCE	1	1	1	8	1	1	51	9	30	—
Single-step regular GPCE	—	—	—	8	1	1	135	9	30	—
	y_0	y_l, l = 1–37	s_k	y_0	y_l, l = 1–37	s_k	y_0	y_l, l = 1–37	s_k	
Example 2										
MPSS-DD-GPCE	1	1	1	2	2	1	63	63	110	—
	1	1	1	3	3	1	93	93	110	—
	2	2	1	3	3	1	498	498	110	—
MPSS-regular-GPCE	—	—	—	2	2	1	198	198	110	—
	—	—	—	3	3	1	858	858	110	—
	y_0	y_1	s_k	y_0	y_1	s_k	y_0	y_1	s_k	
Example 3										
MPSS-DD-GPCE	1	1	2	2	2	2	249	249	9030	1,000,000

[a] The degree of interaction among input variables of the DD-GPCE approximation for an output or score functions.
[b] The total degree or order of the DD-GPCE approximation for an output or a score function.
[c] The sample size of the input-output data set used for estimating expansion coefficients of an output or score function.
[d] The sample size of input-output data set for reliability analysis.

tolerances and initial size parameter are as follows: $\epsilon_1 = 1 \times 10^{-3}$, $\epsilon_2 = 1 \times 10^{-3}$, $\epsilon_3 = 0.01$, $\epsilon_4 = 0.07$, $\epsilon_5 = 0.01$, $\epsilon_6 = 0.5$, $\epsilon_7 = 0.05$, $\epsilon_8 = 1 \times 10^{-4}$, and $\beta_k^{(1)} = 0.3,\ k = 1, \ldots, M$, in Examples 2 and 3.

6.1 Example 1: Optimization of a Mathematical Function

Consider a mathematical problem involving a two-dimensional Gaussian random vector $\mathbf{X} = (X_1, X_2)^\intercal$ with dependent components, which have means $\mathbb{E}_{\mathbf{d}}[X_1] = d_1$ and $\mathbb{E}_{\mathbf{d}}[X_2] = d_2$. Given the design vector $\mathbf{d} = (d_1, d_2)^\intercal$, the objective of this example is to

$$\begin{aligned} \min_{\mathbf{d}\in\mathcal{D}} \quad & c_0(\mathbf{d}) := \frac{\sqrt{\text{var}_{\mathbf{d}}[y_0(\mathbf{X})]}}{\sqrt{\text{var}_{\mathbf{d}_0}[y_0(\mathbf{X})]}}, \\ \text{subject to} \quad & c_1(\mathbf{d}) := 3\sqrt{\text{var}_{\mathbf{d}}[y_1(\mathbf{X})]} - \mathbb{E}_{\mathbf{d}}[y_1(\mathbf{X})] \le 0, \\ & 0 \le d_1 \le 10,\ 0 \le d_2 \le 10, \end{aligned} \tag{55}$$

where

$$y_0(\mathbf{X}) = (X_1 - 4)^3 + (X_1 - 3)^8 + (X_2 - 5)^4 + 10 \tag{56}$$

and

$$y_1(\mathbf{X}) = X_1 + X_2 - 6.45 \tag{57}$$

are two random output functions of $\mathbf{X}$. The initial design vector $\mathbf{d}_0 = (5, 5)^\intercal$. The approximate optimal solution is denoted by $\tilde{\mathbf{d}}^* = (\tilde{d}_1^*, \tilde{d}_2^*)^\intercal$.

Two distinct cases of dependent variables, demonstrating the respective needs of the shifting (Case 1) and scaling (Case 2) transformations, were examined as follows.

Case 1: The standard deviations of X_1 and X_2 are the same as 0.4. The correlation coefficient between X_1 and X_2 is 0.4.

Case 2: The standard deviations of X_1 and X_2 are $0.15d_1$ and $0.15d_2$, respectively. The correlation coefficient between X_1 and X_2 is –0.5.

A former version of this example, originally studied by the authors [29], was slightly revised by increasing the order of y_0.

Table 2 summarizes the approximate optimal solutions for Cases 1 and 2, including the requisite numbers of design iterations and function evaluations, by the single-step, univariate ($S = 1$) DD-GPCE methods. For comparison, the approximate solutions by the single-step regular GPCE methods are included in the third column from the left in Table 2. In addition, the exact solution, obtained from the exact analytical representations of objective and constraint functions and their design sensitivities, are tabulated in the fourth column. In the second and third columns from the left of Table 2, all DD-GPCE- or regular GPCE-based design methods deliver almost identical optimal solutions to the exact one for Cases 1 and 2, all indicating that the constraint is active ($c_1 \simeq 0$). This is possible as the selected order $(m = 8)$ of each DD-GPCE or regular GPCE approximation is the same as those of the original y_0 and y_1. Furthermore, both y_0 and y_1 are effectively univariate functions with no interactions between random variables. Thus, these DD-GPCE and regular GPCE approximations reproduce y_0 and y_1 exactly. Furthermore, both y_0 and y_1 are

TABLE 2: Optimization results of mathematical formulations (Example 1)

Results	Single-step DD-GPCE[a]	Single-step regular GPCE[b]	Exact[c]
Case 1 (shifting)			
$\tilde{d}_1^*$	3.0713	3.0713	3.0700
$\tilde{d}_2^*$	5.3867	5.3867	5.3880
$c_0(\tilde{\mathbf{d}}^*)$	0.0016	0.0016	0.0016
$c_1(\tilde{\mathbf{d}}^*)$	2.7466×10^{-7}	2.7454×10^{-7}	-7.9936×10^{-15}
$\sqrt{\text{var}_{\tilde{\mathbf{d}}^*}[y_0(\mathbf{X})]}$	1.9014	1.9014	1.9014
No. of iterations	15	15	7
No. of y_0 evaluations	51	135	—
No. of y_1 evaluations	9	9	—
Case 2 (scaling)			
$\tilde{d}_1^*$	3.2026	3.2026	3.2017
$\tilde{d}_2^*$	5.3434	5.3434	5.3449
$c_0(\tilde{\mathbf{d}}^*)$	0.0009	0.0009	0.0009
$c_1(\tilde{\mathbf{d}}^*)$	-4.2406×10^{-7}	-4.2069×10^{-7}	2.3843×10^{-7}
$\sqrt{\text{var}_{\tilde{\mathbf{d}}^*}[y_0(\mathbf{X})]}$	8.6253	8.6260	8.6031
No. of iterations	10	10	7
No. of y_0 evaluations	51	135	—
No. of y_1 evaluations	9	9	—

[a] The univariate ($S = 1$), eighth-order ($m = 8$) DD-GPCE approximation was employed for y_0, while the univariate ($S = 1$), first-order ($m = 1$) DD-GPCE was employed for y_1.

[b] The eighth-order ($m = 8$) regular GPCE approximation was employed for y_0, while the first-order ($m = 1$) regular GPCE was employed for y_1.

[c] Exact closed forms of objective, constraint, and their gradient functions were used.

effectively univariate functions with no interactions between random variables. Thus, these DD-GPCE and regular GPCE approximations reproduce y_0 and y_1 exactly.

While the accuracy of both versions of GPCE is excellent, it is important to examine their cost. According to Table 2, the number of y_0 function evaluations for both Cases 1 and 2 required to attain optimal solutions is 51 when the single-step DD-GPCE is employed, which is almost one-third of the 135 function evaluations by the regular GPCE counterpart. This is because the former method is capable of reducing or eliminating the degree of interaction between input variables. In contrast, the latter method should carry all interaction terms of input variables as the order (m) increases. Having said so, both DD-GPCE and regular GPCE approximations at an initial design are adequate for the entire design space. In this case, their coefficients need to be calculated only once during all design iterations. Finally, this example illustrates the merit of the propsed single-step DD-GPCE method over the regular GPCE method in terms of computational efficiency for RDO.

6.2 Example 2: Optimal Sizing Design of a 36-Bar Space Truss Structure

In the second example, a linear-elastic 36-bar space truss, studied by [55], was modified to evaluate the proposed MPSS-DD-GPCE method. As shown in Fig. 4, the truss is simply supported at nodes 1, 2, and 3, and is subjected to a vertically downward concentrated force of 100,000 lb at node 10. The material is aluminum alloy, which has a Young's modulus of 10^7 psi and a mass density of 0.1 lb/in^3. There are 10 ($N = 10$) random variables $\mathbf{X} = (X_1, \ldots, X_{10})^\intercal$, representing random cross-sectional areas of 36 bars, as described in Table 3.

Modeled as correlated Gaussian random variables, for $i, j = 1, \ldots, 10$, they have means $\mathbb{E}_{\mathbf{d}}[X_i]$; standard deviations equal to $0.05\mathbb{E}_{\mathbf{d}}[X_i]$; and correlation coefficients $\rho_{ij} = 0.5$, $i \neq j$. There are ten design variables, as follows: $d_k = \mathbb{E}_{\mathbf{d}}[X_k]$, $k = 1, \ldots, 10$. The objective is to minimize the second-moment properties of the mass of the entire truss structure, constrained by specifying the upper limits of the vertical displacement (v_{10}) at node 10 and axial stresses σ_i, $i = 1, \ldots, 36$, at all 36 bars, such that the limits are satisfied with 99.865% probability if the distribution of each response $y_l(\mathbf{X})$, $l = 1, \ldots, 37$, is standard Gaussian. More specifically, the RDO problem is defined to

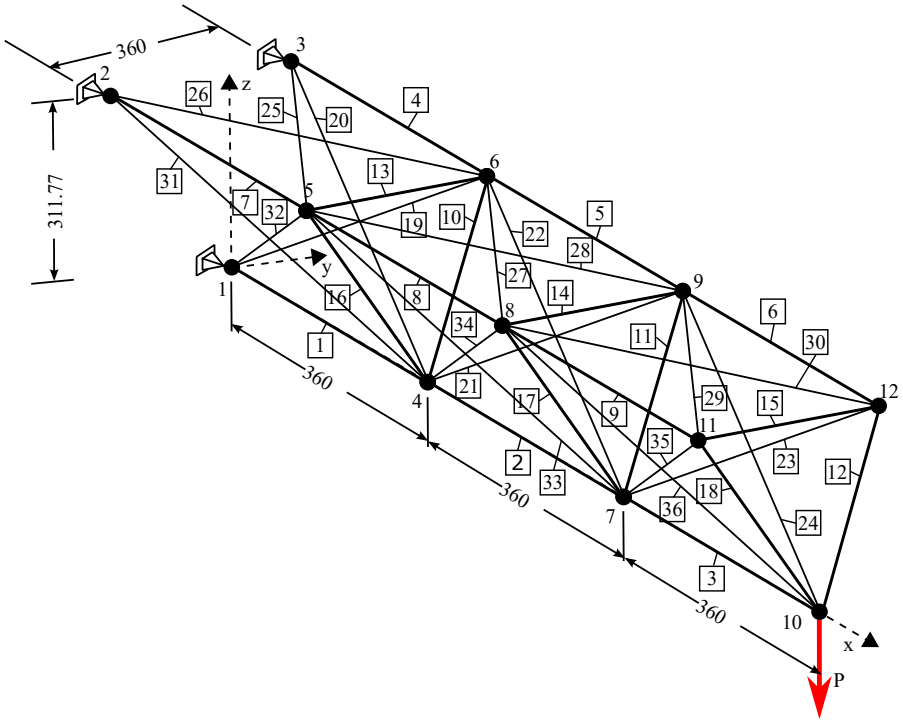

FIG. 4: A 36-bar space truss structure

TABLE 3: Ten random variables X_i, $i = 1, \ldots, 10$, for a 36-bar space truss (Example 2)

Random variables[a] (Cross section areas of bars)	Bar element numbers
X_1	4, 7
X_2	5, 8
X_3	6, 9
X_4	13–15
X_5	1–3
X_6	25–30
X_7	19–24, 31–36
X_8	10, 16
X_9	11, 17
X_{10}	12, 18

[a] Each random variable represents the area of each bar element in the group.

$$\begin{aligned} \min_{\mathbf{d}\in\mathcal{D}\subseteq\mathbb{R}^M} \; & c_0(\mathbf{d}) := 0.5\frac{\mathbb{E}_{\mathbf{d}}[y_0(\mathbf{X})]}{\mathbb{E}_{\mathbf{d}_0}[y_0(\mathbf{x})]} + 0.5\frac{\sqrt{\text{var}_{\mathbf{d}}[y_0(\mathbf{X})]}}{\sqrt{\text{var}_{\mathbf{d}_0}[y_0(\mathbf{X})]}}, \\ \text{subject to } \; & c_l(\mathbf{d}) := 3\sqrt{\text{var}_{\mathbf{d}}[y_l(\mathbf{X})]} - \mathbb{E}_{\mathbf{d}}[y_l(\mathbf{X})] \le 0, \\ & l = 1, \ldots, 37, \\ & 1 \text{ in}^2 \le d_k \le 35 \text{ in}^2, \quad k = 1, \ldots, 10, \end{aligned} \tag{58}$$

where

$$y_0(\mathbf{X}) = 0.1\sum_{i=1}^{10} l_i X_i \tag{59}$$

is the random mass of the truss with l_i, $i = 1, \ldots, 10$, representing bar lengths and

$$y_l(\mathbf{X}) = \begin{cases} 15{,}000 - |\sigma_l(\mathbf{X})|, & \text{if } l = 1, \ldots, 36, \\ 5 - |v_{10}(\mathbf{X})|, & \text{if } l = 37, \end{cases} \tag{60}$$

representing 37 stochastic performance functions. The initial design is $\mathbf{d}_0 = (30, \ldots, 30)^\intercal$ in^2. The approximate optimal solution is denoted by $\tilde{\mathbf{d}}^* = (\tilde{d}_1^*, \ldots, \tilde{d}_{10}^*)^\intercal$.

Table 4 summarizes the assorted results by the proposed MPSS-DD-GPCE and MPSS-regular-GPCE methods. Three approximate optimal designs, presented in the second through fourth columns from the left in Table 4, were obtained by the MPSS-DD-GPCE with the bivariate, third-order ($S = 2$, $m = 3$) approximation; univariate, third-order ($S = 1$, $m = 3$) approximation; and univariate, second-order ($S = 1$, $m = 2$) approximation, respectively.[†] For univariate ($S = 1$) DD-GPCE approximations of the proposed method, the respective optimal designs converge to those by the bivariate ($S = 2$) version as the number of the order (m) increases. For comparison, the optimization results from the MPSS-regular-GPCE method using the third-order ($m = 3$) and the second-order ($m = 2$) approximations for response and score functions, respectively, are tabulated in the fifth and sixth columns of Table 4. All of these optimal designs, obtained by the proposed method and its regular GPCE counterpart, are very close to each other, all satisfying the constraint conditions.

[†] In each case of the design results, the same truncation parameters of the DD-GPCE method were used for objective and constraint functions. Since the objective function is known as a linear function, as shown in Eq. (59), the univariate ($S = 1$), first-order ($m = 1$) DD-GPCE approximation represents the objective function exactly. However, employing higher-variate, higher-order DD-GPCE methods provides solutions identical to those obtained by its linear version for the objective function, which was verified in the case of $S = 2$ and $m = 3$.

TABLE 4: Optimization results of a 36-bar space truss (Example 2)

	MPSS-DD-GPCE			**MPSS-regular-GPCE**		**MCS/FD**[a]	
	S **= 2,** m **= 3**	S **= 1,** m **= 3**	S **= 1,** m **= 2**	m **= 3**	m **= 2**	**I**[b]	**II**[c]
$\tilde{d}_1^*$	20.7079	20.7595	20.2586	20.6944	20.9581	21.8505	21.7180
$\tilde{d}_2^*$	12.2492	12.2663	12.4741	12.2327	12.2326	13.4408	13.3868
$\tilde{d}_3^*$	4.1362	4.1474	4.2172	4.1210	4.6160	3.3252	3.2726
$\tilde{d}_4^*$	1.0000	1.0000	1.0000	1.0000	1.0000	1.0000	1.0000
$\tilde{d}_5^*$	29.3687	29.2770	29.3697	29.4036	29.6739	29.3458	29.6267
$\tilde{d}_6^*$	1.0000	1.0000	1.0000	1.0000	1.0000	1.0000	1.0000
$\tilde{d}_7^*$	6.2517	6.2820	6.2479	6.2527	6.1061	6.0896	6.0700
$\tilde{d}_8^*$	1.0000	1.0000	1.1212	1.0000	1.0895	1.0000	1.0000
$\tilde{d}_9^*$	1.0000	1.0000	1.0000	1.0000	1.0000	1.0000	1.0000
$\tilde{d}_{10}^*$	3.9222	3.6877	4.1921	3.8985	4.2420	3.5590	3.5315
$c_0(\tilde{\mathbf{d}}^*)$	0.2256	0.2256	0.2259	0.2256	0.2259	0.2251	0.2247
$\max[c_l(\tilde{\mathbf{d}}^*)]$[d], l = 1–37	-7.9566×10^{-8}	-1.6147×10^{-7}	-4.3102×10^{-6}	2.0730×10^{-7}	-1.0992×10^{-6}	1.4095×10^{-8}	4.0499×10^{-6}
$\mathbb{E}_{\tilde{\mathbf{d}}^*}[y_0(\mathbf{X})]$, lb	1.0502×10^5	1.0499×10^5	1.0517×10^5	1.0501×10^5	1.0527×10^5	1.0483×10^5	1.0482×10^5
$\sqrt{\text{var}_{\tilde{\mathbf{d}}^*}[y_0(\mathbf{X})]}$, lb	4.1568×10^3	4.1572×10^3	4.1607×10^3	4.1569×10^3	4.1590×10^3	4.1457×10^3	4.1464×10^3
No. of FEA	8466	1209	1008	14,586	2970	157,500,000	96,600,000

[a] Crude MCS with 10^5 sample size for statistical moment and design sensitivity analysis based on the central finite difference method.
[b] The initial design was set to the optimal solution of the MPSS-regular-GPCE ($m = 3$).
[c] The initial design was set to the optimal solution of the MPSS-regular-GPCE ($m = 2$).
[d] The maximum value among constraint values c_l at the optimum $\mathbf{d}^*$, $l = 1, \ldots, 37$.

To seek further credibility for the accuracy of the RDO solutions by the proposed method, QMCS entailing 1×10^5 samples for stochastic moment analysis and design sensitivity analysis based on the central finite-difference method was employed. However, due to its extensive computational cost, the RDO problem was solved for two different initial designs assigned as two optimal designs by the MPSS-regular-GPCE methods, presented in the fifth and sixth columns of Table 4, respectively. The resulting two reference solutions, denoted by MCS/FD I and II for the former and the latter cases of the initial design, respectively, are listed in the seventh and eighth columns of Table 4. As expected, these two reference solutions are very close to their initial designs. However, d_3^* and d_{10}^* show some discrepancy between those solutions obtained by the MPSS methods and MCS/FD. Since the sample size used for these reference solutions is limited due to its high computational cost, such differences need to be further examined. Having said so, these results still indicate that the optimal designs obtained by the MCSS-DD-GPCE methods are accurate and reliable. Furthermore, when compared with hundreds of millions of FEA mandated to obtain reference solutions, both the MPSS-DD-GPCE and MPSS-regular-GPCE methods achieve a dramatic reduction of computational cost, requiring only 1008–14,586 FEA. More importantly, the proposed third-order ($m = 3$) MPSS-DD-GPCE methods of the univariate ($S = 1$) and bivariate ($S = 2$) approximations require only 1209 and 8466 FEA to obtain the converged optimal design, while the third-order ($m = 3$) regular GPCE counterpart demands 14,586 FEA. Therefore, the proposed MPSS-DD-GPCE method is not only accurate but also more computationally efficient than the MPSS-regular-GPCE method in solving this practical RDO problem.

6.3 Example 3: Shape Optimization of a Train Bogie Side Frame

The last example establishes the efficacy of the proposed MPSS-DD-GPCE method in designing an industrial-scale mechanical component, known as a train bogie side frame. In rail vehicles, a bogie usually remains affixed to a railway carriage or locomotive. As illustrated in Fig 5(a), a four-wheeled bogie provides support for the vehicle body and is also used to provide its traction and braking. The bogie side frame is a chassis or framework that carries wheels affixed to the train, serving as a modular subassembly of wheels and axles to provide some degree of cushioning against severe stresses and shocks transmitted from the track during the train motion. Therefore, the bogie side frame should be designed to possess adequate fatigue durability under multiple loading conditions, including longitudinal, lateral, or vertical loading, and must sustain satisfactory performances during its expected service lifetime. However, any uncertainties arising in material properties or manufacturing variables, if they exist, result in the randomness of fatigue life. A traditional deterministic design optimization incorporating large safety factors may lead to increased weight of a vehicle, causing a loss of fuel efficiency. Therefore, incorporating uncertainty in fatigue life under multiple loading conditions is essential for creating a lightweight bogie side frame design.

Forty-one input random variables were introduced to model the randomness in manufacturing tolerances of the bogie side frame geometry. Figure 5(b) depicts a computer-aided design (CAD) model of a bogie side frame with 41 random manufacturing variables X_k, $k = 1, \ldots, 41$, which are marked in the front and isometric views.

For $k = 1, \ldots, 41$, the random variables follow a multivariate lognormal distribution with the means $\mathbb{E}_{\mathbf{d}}[\mathbf{X}_k]$ and standard deviations $0.02\mathbb{E}_{\mathbf{d}}[\mathbf{X}_k]$. These random variables are correlated with each other with a correlation coefficient of 0.4. There are 41 design variables, such that $d_k = \mathbb{E}_{\mathbf{d}}[\mathbf{X}_k]$, $k = 1, \ldots, 41$. The bogie side frame is made of cast steel with the following deterministic material properties: elastic modulus $E = 203$ GPa, Poisson's ratio $\nu = 0.3$, mass density $\rho = 7800$ kg/m^3, fatigue strength coefficient $\sigma'_f = 1332$ MPa, fatigue ductility coefficient $\epsilon'_f = 0.375$, fatigue strength exponent $b = -0.1085$, and fatigue ductility exponent $c = -0.6354$.

The stochastic performance of the bogie side frame was determined by fatigue durability analysis under a vertical loading condition F on the rectangular surface of the bottom side of the center holes of the frame, as shown in Fig. 6(a). The loading condition is created when the train body with a mass of 500 tons is subject to a vertical acceleration of 1 g by the gravity force or a vertical acceleration of 1.4 g by the gravity force and a vertical crush load due to track-induced forces in the train motion. As a result, the bogie side frame experiences constant-amplitude cyclic loads with the maximum and minimum load values as follows: 2452.5 kN (1 g) $\leq F \leq$ 3433.5 kN (1.4 g). The essential boundary condition includes fixing the inner surface of the two arms in the three translational directions. The fatigue durability analysis involved (1) calculating maximum principal strain and mean stress at a critical point; and (2) calculating the fatigue crack-initiation life at the critical point from the Coffin-Manson-Morrow equation [56].

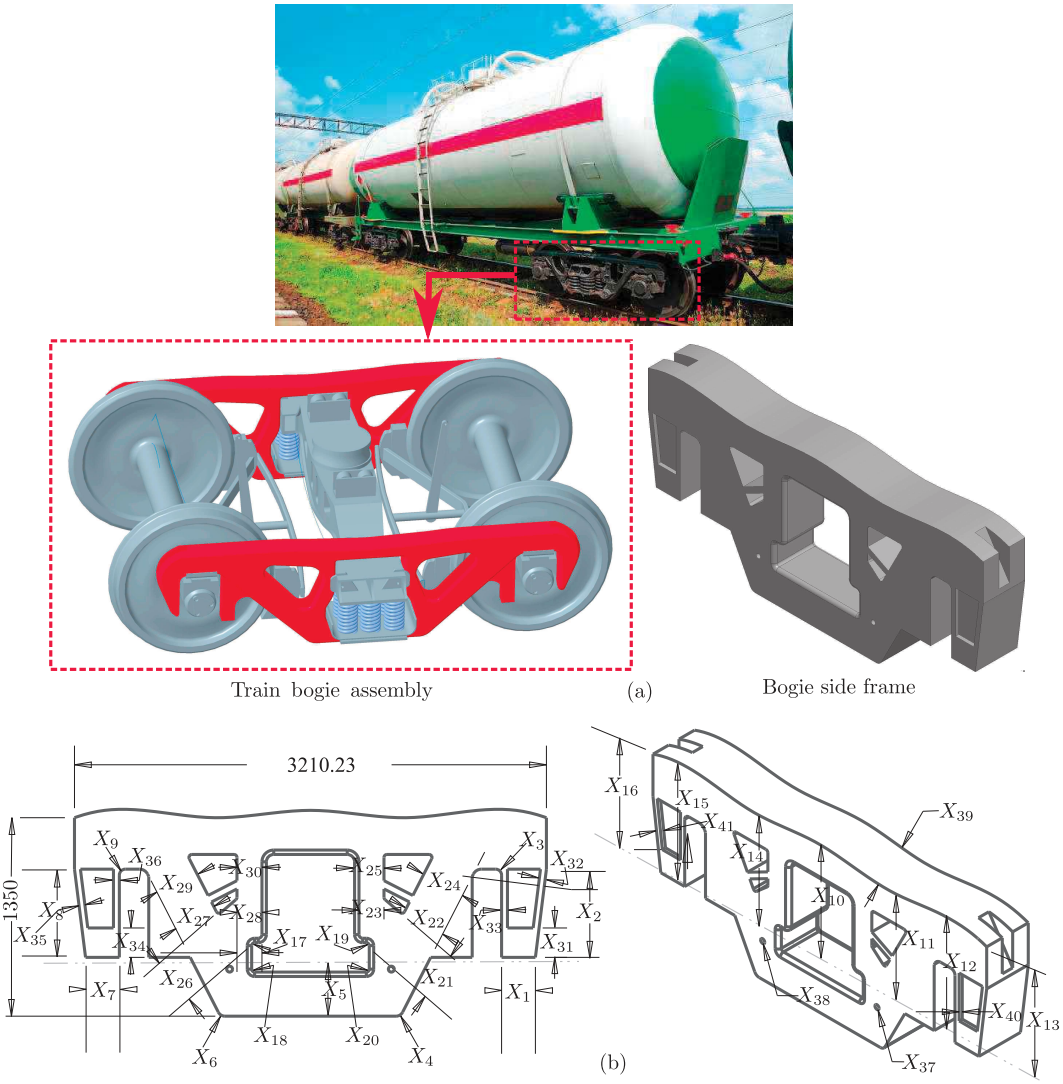

FIG. 5: A train bogie side frame (Example 3); (a) a photo of the train bogie assembly; (b) a CAD model of the bogie side frame (unit: mm)

The critical point is where the von Mises stress is the largest, provided that the maximum principal stress is tensile. Such point location is nonstationary due to the random geometry; thus the critical point was identified from FEA at each design iteration.

The objective is to minimize the mean mass of the bogie side frame by changing the geometry such that its fatigue crack-initiation life $N_1(\mathbf{X})$ at the critical point under the cyclic loading condition F must exceed a design threshold of 10 million cycles with $(1-\Phi(-3))\times 100 = 99.865\%$ probability, where $\Phi(\cdot)$ is the standard normal distribution function. Mathematically, the RBDO for this problem is defined as

$$\begin{aligned} \min_{\mathbf{d}\in\mathcal{D}} \ & c_0(\mathbf{d}) := \frac{\mathbb{E}_{\mathbf{d}}[y_0(\mathbf{X})]}{\mathbb{E}_{\mathbf{d}_0}[y_0(\mathbf{X})]}, \\ \text{subject to } & c_1(\mathbf{d}) := \mathbb{P}_{\mathbf{d}}[y_1(\mathbf{X})<0] - \Phi(-3) \le 0, \\ & d_{k,L} \le d_k \le d_{k,U}, \quad k=1,\dots,41, \end{aligned} \tag{61}$$

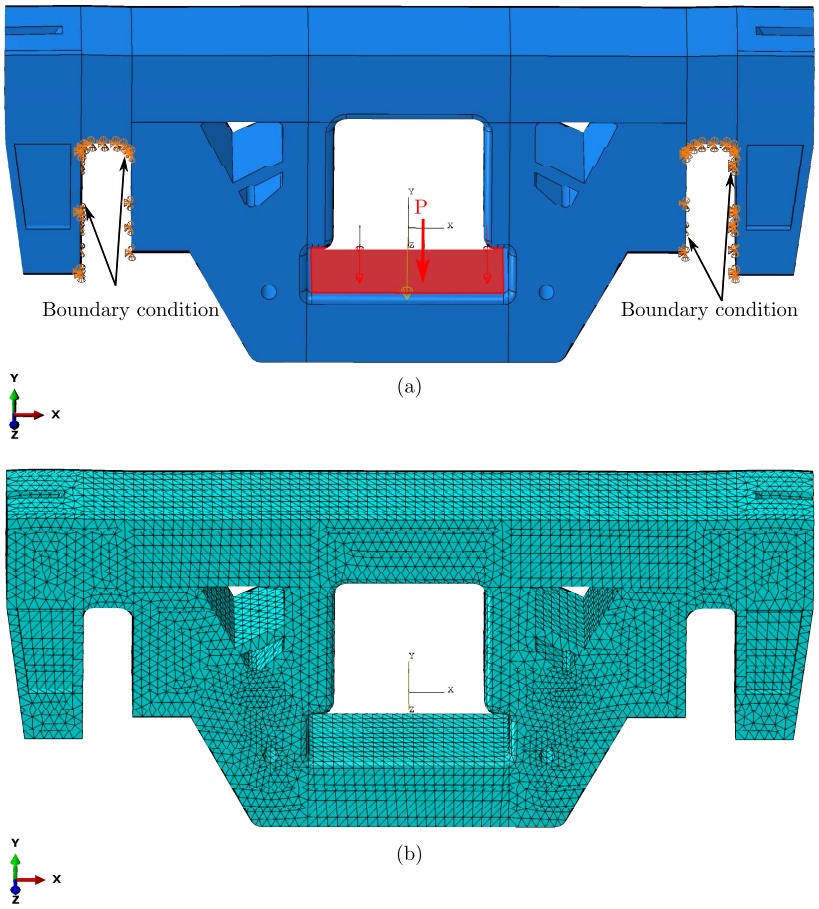

FIG. 6: An FEA of the bogie side frame (Example 3); (a) vertical load and boundary conditions; (b) a tetrahedral mesh comprising 157,647 elements

where

$$y_0(\mathbf{X}) = \rho \int_{\mathcal{D}'(\mathbf{X})} d\mathcal{D}' \tag{62}$$

is the random mass of the bogie side frame, and

$$y_1(\mathbf{X}) = \log\left[\frac{N_1(\mathbf{X})}{1 \times 10^7}\right] \tag{63}$$

is a stochastic performance function given by the log-scale normalized fatigue crack-initiation life for the bogie side frame. The initial design $\mathbf{d}_0 = (d_{1,0}, \ldots, d_{41,0})^\intercal$; the upper and lower bounds of the design vector $\mathbf{d} = (d_1, \ldots, d_{41})^\intercal$ mm $\in \mathcal{D} \subset \mathbb{R}^{41}$ are tabulated in Table 5. Figure 6(b) presents an FEA mesh for the bogie side frame at mean input and initial design, which comprises 157,647 tetrahedral elements. The approximate optimal solution is denoted by $\tilde{\mathbf{d}}^* = (\tilde{d}_1^*, \ldots, \tilde{d}_{41}^*)^\intercal$.

The MPSS-DD-GPCE method with the univariate, second-order ($S = 1$, $m = 2$) DD-GPCE approximation was employed in solving this RBDO problem. The obtained optimal design solutions are tabulated in the third column from the left in Table 5. At optimum, d_3 and d_{10}–d_{16} almost reached their lower limits, and the rest of the design variables are between their lower and upper limits, satisfying an almost active constraint $c_1 \simeq -5.06 \times 10^{-4}$. The mean mass of the optimal bogie side frame is 4.2169 tons, which presents a 50.39% reduction from the initial mean mass of 8.5008 tons. To complete the design process, the requisite number of FEA is 4980.

TABLE 5: Initial and optimal values, and bounds of design variables for the bogie side frame problem (Example 3)

k	$d_{l,0}$ mm	$\tilde{d}_l^*$ mm	$d_{l,L}$ mm	$d_{l,U}$ mm
1	230	95.04	80	250
2	600	437.76	400	600
3	40	30.04	30	50
4	50	81.37	50	100
5	500	332.97	330	500
6	50	94.28	50	100
7	230	146.89	80	250
8	600	448.10	400	600
9	40	46.62	30	50
10	900	850.84	850	900
11	900	752.84	750	900
12	900	801.72	800	900
13	900	851.16	850	900
14	900	752.79	750	900
15	900	801.69	800	900
16	900	851.80	850	900
17	20	19.58	10	30
18	20	18.33	10	50
19	20	12.20	10	30
20	20	27.04	10	50
21	300	170.60	100	300
22	300	203.32	100	300
23	200	160.09	100	200
24	300	150.33	100	300
25	200	122.40	100	200
26	300	181.59	100	300
27	300	230.82	100	300
28	200	125.28	100	200
29	300	113.75	100	300
30	200	104.39	100	200
31	200	186.15	100	200
32	40	37.62	20	40
33	40	39.58	20	40
34	200	193.06	100	200
35	40	30.81	20	40
36	40	33.92	20	40
37	30	39.43	30	40
38	30	38.44	30	40
39	400	301.69	300	400
40	30	41.85	30	60
41	30	39.05	30	60

Figures 7(a)–7(d) present the contour plots of the logarithm of the fatigue crack-initiation life at the mean shapes of the bogie side frame for several design iterations (q'), including the initial design and the optimal design. The RBDO process started with a conservative initial design such that its minimum fatigue crack-initiation life of 2.11×10^{15} cycles is much larger than the target value of 10^7 cycles. Through the proposed method with tolerances and

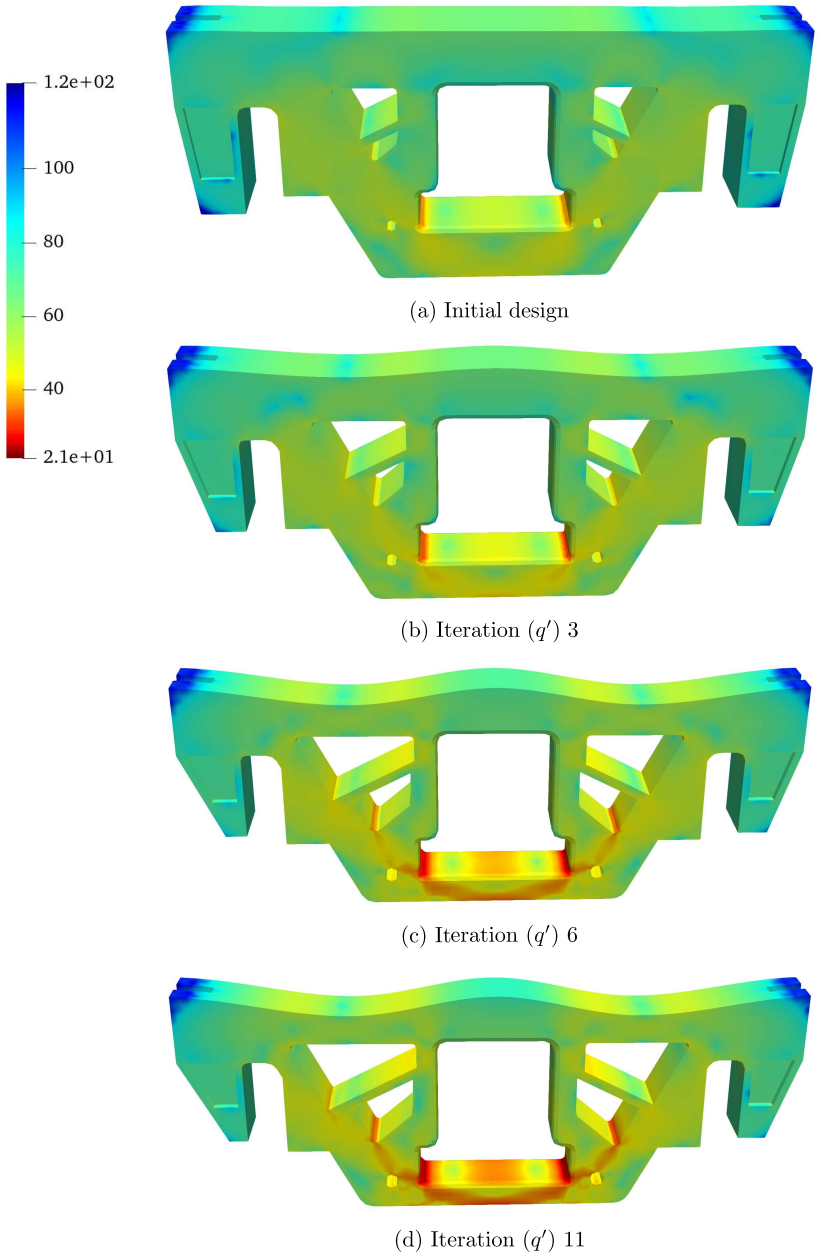

(a) Initial design

(b) Iteration (q') 3

(c) Iteration (q') 6

(d) Iteration (q') 11

FIG. 7: Contours of logarithmic fatigue crack-initiation life at the mean shapes of the bogie side frame (Example 3): (a) initial design; (b) iteration (q') 3; (c) iteration (q') 6; (d) iteration (q') 11 (optimum), obtained from the MPSS-DD-GPCE method with the univariate, second-order ($S = 1$, $m = 2$) approximation

subregion size parameters appropriately selected, a total of 11 iterations (q') led to a final optimal design. Indeed, at optimum, there is a considerable reduction in the overall volume of the bogie side frame, satisfying the target fatigue crack-initiation life, as presented in Fig. 7(d). Consequently, the minimum weight and target reliability of the bogie side frame were both achieved, a distinctive advantage of RBDO over traditional deterministic design optimization. This culminating example confirms that the proposed RBDO method is capable of solving industrial-scale engineering design problems using only a few thousand FEA.

7. CONCLUSIONS

Two innovative reconfigurations of GPCE, leading to the single-step DD-GPCE method and the MPSS-DD-GPCE method, were invented for high-dimensional stochastic design optimization of complex mechanical systems in the presence of input random variables with arbitrary, dependent probability distributions. The methods feature the DD-GPCE approximation for statistical moment and reliability analyses of a high-dimensional stochastic response; a novel synthesis between DD-GPCE and score functions for estimating the first-order design sensitivities of the statistical moments and failure probability; and a standard gradient-based optimization algorithm, constructing single-step DD-GPCE and MPSS-DD-GPCE methods. In these new design methods, the multivariate orthonormal basis functions are built consistent with the desired degree of interaction between input variables and the polynomial order, thus helping to alleviate the curse of dimensionality to a substantial magnitude. In addition, when integrated with score functions, the DD-GPCE approximation leads to analytical formulae for calculating the design sensitivities. More significantly, the statistical moments, failure probability, and their respective design sensitivities are determined concurrently from a single stochastic analysis or simulation.

Of the two design methods developed, the single-step DD-GPCE method, formulated globally on the entire design space, is highly efficient due to recycling of the expansion coefficients. However, it may not remain accurate or effective when confronted with overly large design spaces and/or high-dimensional stochastic responses. In contrast, the MPSS-DD-GPCE method ushers in a local enforcement of DD-GPCE approximations, where the original RDO or RBDO problem is converted into a series of concomitant local problems defined on subregions of the entire design space. As a result, the method allows employing a low-degree DD-GPCE approximation to obtain a reliable design solution even when a design space is large. Also, the latter method avoids the necessity of recomputing the expansion coefficients by reprocessing the old expansion coefficients whenever possible, thus dramatically reducing the computational cost. Therefore, the MPSS-DD-GPCE method is capable of solving practical engineering problems, as demonstrated by shape design optimization of an industrial-scale bogie side frame with 41 random variables.

ACKNOWLEDGMENT

This research was supported by the U.S. National Science Foundation (Grant No. CMMI-1933114).

REFERENCES

1. Kuschel, N. and Rackwitz, R., Two Basic Problems in Reliability-Based Structural Optimization, *Math. Methods Ope. Res.*, **46**(3):309–333, 1997.
2. Tu, J., Choi, K.K., and Park, Y.H., A New Study on Reliability-Based Design Optimization, *J. Mech. Des.*, **121**(4):557–564, 1999.
3. Du, X. and Chen, W., Sequential Optimization and Reliability Assessment Method for Efficient Probabilistic Design, *J. Mech. Des.*, **126**(2):225–233, 2004.
4. Chiralaksanakul, A. and Mahadevan, S., First-Order Approximation Methods in Reliability-Based Design Optimization, *J. Mech. Des.*, **127**(5):851–857, 2004.
5. Agarwal, H. and Renaud, J.E., New Decoupled Framework for Reliability-Based Design Optimization, *AIAA J.*, **44**(7):1524–1531, 2006.
6. Liang, J., Mourelatos, Z.P., and Nikolaidis, E., A Single-Loop Approach for System Reliability-Based Design Optimization, *J. Mech. Des.*, **129**(12):1215–1224, 2007.
7. Rahman, S. and Wei, D., Design Sensitivity and Reliability-Based Structural Optimization by Univariate Decomposition, *Struct. Multidiscipl. Optim.*, **35**(3):245–261, 2008.
8. Ren, X., Yadav, V., and Rahman, S., Reliability-Based Design Optimization by Adaptive-Sparse Polynomial Dimensional Decomposition, *Struct. Multidiscipl. Optim.*, **53**(3):425–452, 2016.
9. Lee, D. and Rahman, S., Reliability-Based Design Optimization under Dependent Random Variables by a Generalized Polynomial Chaos Expansion, *Struct. Multidiscipl. Optim.*, **65**(1):1–29, 2022.
10. Hassan, R. and Crossley, W., Spacecraft Reliability-Based Design Optimization under Uncertainty Including Discrete Variables, *J. Spacecr. Rockets*, **45**(2):394–405, 2008.

11. Nannapaneni, S. and Mahadevan, S., Probability-Space Surrogate Modeling for Fast Multidisciplinary Optimization under Uncertainty, *Reliab. Eng. System Saf.*, **198**:106896, 2020.
12. Youn, B.D., Choi, K., Yang, R.J., and Gu, L., Reliability-Based Design Optimization for Crashworthiness of Vehicle Side Impact, *Struct. Multidiscipl. Optim.*, **26**(3):272–283, 2004.
13. Gu, X., Lu, J., and Wang, H., Reliability-Based Design Optimization for Vehicle Occupant Protection System Based on Ensemble of Metamodels, *Struct. Multidiscipl. Optim.*, **51**(2):533–546, 2015.
14. Siavashi, S. and Eamon, C.D., Development of Traffic Live-Load Models for Bridge Superstructure Rating with RBDO and Best Selection Approach, *J. Bridge Eng.*, **24**(8):04019084, 2019.
15. Kang, B., Choi, K., and Kim, D.H., An Efficient Serial-Loop Strategy for Reliability-Based Robust Optimization of Electromagnetic Design Problems, *IEEE Trans. Magn.*, **54**(3):1–4, 2017.
16. Li, L., Wan, H., Gao, W., Tong, F., and Li, H., Reliability Based Multidisciplinary Design Optimization of Cooling Turbine Blade Considering Uncertainty Data Statistics, *Struct. Multidiscipl. Optim.*, **59**(2):659–673, 2019.
17. Youn, B.D. and Choi, K.K., A New Response Surface Methodology for Reliability-Based Design Optimization, *Comput. Struct.*, **82**(2-3):241–256, 2004.
18. Suryawanshi, A. and Ghosh, D., Reliability Based Optimization in Aeroelastic Stability Problems Using Polynomial Chaos Based Metamodels, *Struct. Multidiscipl. Optim.*, **53**(5):1069–1080, 2016.
19. Eldred, M.S. and Elman, H.C., Design under Uncertainty Employing Stochastic Expansion Methods, *Int. J. Uncertainty Quantif.*, **1**(2):119–146, 2011.
20. Yang, I.T. and Hsieh, Y.H., Reliability-Based Design Optimization with Cooperation between Support Vector Machine and Particle Swarm Optimization, *Eng. Comput.*, **29**(2):151–163, 2013.
21. Lehkỳ, D., Slowik, O., and Novák, D., Reliability-Based Design: Artificial Neural Networks and Double-Loop Reliability-Based Optimization Approaches, *Adv. Eng. Software*, **117**:123–135, 2018.
22. Zhao, L., Choi, K., and Lee, I., Metamodeling Method Using Dynamic Kriging for Design Optimization, *AIAA J.*, **49**(9):2034–2046, 2011.
23. Emmerich, M.T., Giannakoglou, K.C., and Naujoks, B., Single and Multiobjective Evolutionary Optimization Assisted by Gaussian Random Field Metamodels, *IEEE Trans. Evol. Comput.*, **10**(4):421–439, 2006.
24. Kouri, D.P. and Shapiro, A., Optimization of PDEs with Uncertain Inputs, in *Frontiers in PDE-Constrained Optimization*, pp. 41–81, Berlin: Springer, 2018.
25. Kolvenbach, P., Lass, O., and Ulbrich, S., An Approach for Robust PDE-Constrained Optimization with Application to Shape Optimization of Electrical Engines and of Dynamic Elastic Structures under Uncertainty, *Optim. Eng.*, **19**(3):697–731, 2018.
26. Conti, S., Held, H., Pach, M., Rumpf, M., and Schultz, R., Shape Optimization under Uncertainty—A Stochastic Programming Perspective, *SIAM J. Optim.*, **19**(4):1610–1632, 2009.
27. Noh, Y., Choi, K., and Du, L., Reliability-Based Design Optimization of Problems with Correlated Input Variables Using a Gaussian Copula, *Struct. Multidiscipl. Optim.*, **38**(1):1–16, 2009.
28. Lee, I., Choi, K.K., Noh, Y., Zhao, L., and Gorsich, D., Sampling-Based Stochastic Sensitivity Analysis Using Score Functions for RBDO Problems with Correlated Random Variables, *J. Mech. Des.*, **133**(2):021003, 2011.
29. Lee, D. and Rahman, S., Robust Design Optimization under Dependent Random Variables by a Generalized Polynomial Chaos Expansion, *Struct. Multidiscipl. Optim.*, **63**(5):2425–2457, 2021.
30. Navarro, M., Witteveen, J., and Blom, J., Polynomial Chaos Expansion for General Multivariate Distributions with Correlated Variables, *Math. Numer. Anal.*, arXiv:1406.5483, 2014.
31. Jakeman, J.D., Franzelin, F., Narayan, A., Eldred, M., and Plfger, D., Polynomial Chaos Expansions for Dependent Random Variables, *Comput. Methods Appl. Mech. Eng.*, **351**:643–666, 2019.
32. Rahman, S., A Polynomial Chaos Expansion in Dependent Random Variables, *J. Math. Anal. Appl.*, **464**(1):749–775, 2018.
33. Lee, D. and Rahman, S., Practical Uncertainty Quantification Analysis Involving Statistically Dependent Random Variables, *Appl. Math. Modell.*, **84**:324–356, 2020.
34. Zuniga, M.M., Kucherenko, S., and Shah, N., Metamodelling with Independent and Dependent Inputs, *Comput. Phys. Commun.*, **184**(6):1570–1580, 2013.
35. Rahman, S., Uncertainty Quantification under Dependent Random Variables by a Generalized Polynomial Dimensional Decomposition, *Comput. Methods Appl. Mech. Eng.*, **344**:910–937, 2019.

36. Kriegesmann, B., Robust Design Optimization with Design-Dependent Random Input Variables, *Struct. Multidiscipl. Optim.*, **61**(2):661–674, 2020.
37. Toropov, V., Filatov, A., and Polynkin, A., Multiparameter Structural Optimization Using FEM and Multipoint Explicit Approximations, *Struct. Multidiscipl. Optim.*, **6**(1):7–14, 1993.
38. Kang, K., Kim, S.W., Yoon, K., and Choi, D.H., Robust Design Optimization of an Angular Contact Ball Bearing under Manufacturing Tolerance, *Struct. Multidiscipl. Optim.*, **60**(4):1645–1665, 2019.
39. Chunyan, L., Jingzhe, L., and Way, K., Bayesian Support Vector Machine for Optimal Reliability Design of Modular Systems, *Reliab. Eng. Syst. Saf.*, **228**:108840, 2022.
40. Lee, I., Choi, K., and Zhao, L., Sampling-Based RBDO Using the Stochastic Sensitivity Analysis and Dynamic Kriging Method, *Struct. Multidiscipl. Optim.*, **44**(3):299–317, 2011.
41. Uryasev, S., Derivatives of Probability Functions and Some Applications, *Ann. Oper. Res.*, **56**(1):287–311, 1995.
42. Van Ackooij, W. and Henrion, R., Gradient Formulae for Nonlinear Probabilistic Constraints with Gaussian and Gaussian-Like Distributions, *SIAM J. Optim.*, **24**(4):1864–1889, 2014.
43. Farshbaf-Shaker, M.H., Henrion, R., and Hömberg, D., Properties of Chance Constraints in Infinite Dimensions with an Application to PDE Constrained Optimization, *Set-Valued Variational Anal.*, **26**(4):821–841, 2018.
44. Ren, X. and Rahman, S., Stochastic Design Optimization Accounting for Structural and Distributional Design Variables, *Eng. Comput.*, **35**(8):2654–2695, 2018.
45. Chen, W., Allen, J., Tsui, K., and Mistree, F., Procedure for Robust Design: Minimizing Variations Caused by Noise Factors and Control Factors, *J. Mech. Des.*, **118**(4):478–485, 1996.
46. Du, X. and Chen, W., Towards a Better Understanding of Modeling Feasibility Robustness in Engineering Design, *J. Mech. Des.*, **122**(4):385–394, 2000.
47. Ren, X. and Rahman, S., Robust Design Optimization by Polynomial Dimensional Decomposition, *Struct. Multidiscipl. Optim.*, **48**(1):127–148, 2013.
48. Rahman, S., Dimensionwise Multivariate Orthogonal Polynomials in General Probability Spaces, *Appl. Math. Comput.*, **362**:124538, 2019.
49. Rahman, S., A Generalized ANOVA Dimensional Decomposition for Dependent Probability Measures, *SIAM/ASA J. Uncertainty Quantif.*, **2**(1):670–697, 2014.
50. Browder, A., *Mathematical Analysis: An Introduction*, Undergraduate Texts in Mathematics, Berlin: Springer Verlag, 1996.
51. Rubinstein, R. and Shapiro, A., *Discrete Event Systems: Sensitivity Analysis and Stochastic Optimization by the Score Function Method*, New York: Wiley, 1993.
52. Rahman, S., Stochastic Sensitivity Analysis by Dimensional Decomposition and Score Functions, *Probab. Eng. Mech.*, **24**(3):278–287, 2009.
53. Busbridge, I., Some Integrals Involving Hermite Polynomials, *J. London Math. Soc.*, **23**:135–141, 1948.
54. Rahman, S. and Ren, X., Novel Computational Methods for High-Dimensional Stochastic Sensitivity Analysis, *Int. J. Numer. Methods Eng.*, **98**(12):881–916, 2014.
55. Kiran, R., Li, L., and Khandelwal, K., Complex Perturbation Method for Sensitivity Analysis of Nonlinear Trusses, *J. Struct. Eng.*, **143**(1):04016154, 2017.
56. Stephens, R., Fatemi, A., Stephens, R.R., and Fuchs, H., *Metal Fatigue in Engineering*, New York: Wiley-Interscience, 2000.
57. Xiu, D. and Karniadakis, G.E., The Wiener-Askey Polynomial Chaos for Stochastic Differential Equations, *SIAM J. Sci. Comput.*, **24**:619–644, 2002.
58. Wiener, N., The Homogeneous Chaos, *Am. J. Math.*, **60**(4):897–936, 1938.

APPENDIX A. GENERALIZED POLYNOMIAL CHAOS EXPANSION

Let $\mathbf{j} := (j_1, \ldots, j_N) \in \mathbb{N}_0^N$ be an N-dimensional multi-index. For $\mathbf{z} = (z_1, \ldots, z_N)^\intercal \in \bar{\mathbb{A}}^N \subseteq \mathbb{R}^N$, a monomial in the real variables $z_1, \ldots, z_N$ is the product $\mathbf{z}^\mathbf{j} = z_1^{j_1} \ldots z_N^{j_N}$ with a total degree $|\mathbf{j}| = j_1 + \ldots + j_N$. Consider for each $m \in \mathbb{N}_0$ the elements of the multi-index set

$$\mathcal{J}_m := \{\mathbf{j} \in \mathbb{N}_0^N : |\mathbf{j}| \le m\},$$

which is arranged as $\mathbf{j}^{(1)}, \ldots, \mathbf{j}^{(L_{N,m})}$, $\mathbf{j}^{(1)} = \mathbf{0}$, according to a monomial order of choice. The set $\mathcal{J}_m$ has cardinality $L_{N,m}$ obtained as

$$L_{N,m} := |\mathcal{J}_m| = \sum_{l=0}^{m} \binom{N+l-1}{l} = \binom{N+m}{m}. \tag{A.1}$$

Denote by

$$\mathbf{\Psi}_m(\mathbf{z};\mathbf{g}) = (\Psi_1(\mathbf{z};\mathbf{g}), \ldots, \Psi_{L_{N,m}}(\mathbf{z};\mathbf{g}))^\intercal \tag{A.2}$$

an $L_{N,m}$-dimensional vector of multivariate orthonormal polynomials that is consistent with the probability measure $f_{\mathbf{Z}}(\mathbf{z};\mathbf{g})d\mathbf{z}$ of $\mathbf{Z}$. It is determined by the following three steps [29,33].

Step 1. Given $m \in \mathbb{N}_0$, create an $L_{N,m}$-dimensional column vector

$$\mathbf{P}_m(\mathbf{z}) = (\mathbf{z}^{\mathbf{j}^{(1)}}, \ldots, \mathbf{z}^{\mathbf{j}^{(L_{N,m})}})^\intercal, \tag{A.3}$$

whose elements are the monomials $\mathbf{z}^{\mathbf{j}}$ for $|\mathbf{j}| \leq m$ arranged in the aforementioned order. It is referred to as the monomial vector in $\mathbf{z} = (z_1, \ldots, z_N)^\intercal$ of degree at most m.

Step 2. Construct an $L_{N,m} \times L_{N,m}$ monomial moment matrix of $\mathbf{P}_m(\mathbf{Z})$, defined as

$$\begin{aligned} \mathbf{G}_m &:= \mathbb{E}_{\mathbf{g}}[\mathbf{P}_m(\mathbf{Z})\mathbf{P}_m^\intercal(\mathbf{Z})] \\ &:= \int_{\bar{\mathbb{A}}^N} \mathbf{P}_m(\mathbf{z})\mathbf{P}_m^\intercal(\mathbf{z}) f_{\mathbf{Z}}(\mathbf{z};\mathbf{g}) d\mathbf{z}. \end{aligned} \tag{A.4}$$

For an arbitrary PDF $f_{\mathbf{Z}}(\mathbf{z};\mathbf{g})$, $\mathbf{G}_m$ cannot be determined exactly, but it can be estimated with good accuracy by numerical integration or sampling methods [33].

Step 3. Select the $L_{N,m} \times L_{N,m}$ whitening matrix $\mathbf{W}_m$ from the Cholesky decomposition of the monomial moment matrix $\mathbf{G}_m$ such that

$$\mathbf{W}_m^\intercal \mathbf{W}_m = \mathbf{G}_m^{-1} \text{ or } \mathbf{W}_m^{-1}\mathbf{W}_m^{-\intercal} = \mathbf{G}_m. \tag{A.5}$$

Then, employ the whitening transformation to generate multivariate orthonormal polynomials from

$$\mathbf{\Psi}_m(\mathbf{z};\mathbf{g}) = \mathbf{W}_m \mathbf{P}_m(\mathbf{z}). \tag{A.6}$$

For an ith element $\Psi_i(\mathbf{Z};\mathbf{g})$ of the polynomial vector $\mathbf{\Psi}_m(\mathbf{Z};\mathbf{g}) = (\Psi_1(\mathbf{Z};\mathbf{g}), \ldots, \Psi_{L_{N,m}}(\mathbf{Z};\mathbf{g}))^\intercal$, the first- and second-order moments are [33]

$$\mathbb{E}_{\mathbf{g}}[\Psi_i(\mathbf{Z};\mathbf{g})] = \begin{cases} 1, & \text{if } i = 1, \\ 0, & \text{if } i \neq 1, \end{cases} \tag{A.7}$$

and

$$\mathbb{E}_{\mathbf{g}}[\Psi_i(\mathbf{Z};\mathbf{g})\Psi_j(\mathbf{Z};\mathbf{g})] = \begin{cases} 1, & i = j, \\ 0, & i \neq j, \end{cases} \tag{A.8}$$

respectively.

According to Eqs. (A.7) and (A.8), any two distinct elements $\Psi_i(\mathbf{z};\mathbf{g})$ and $\Psi_j(\mathbf{z};\mathbf{g})$, $i, j = 1, \ldots, L_{N,m}$, of the polynomial vector $\mathbf{\Psi}_m(\mathbf{z};\mathbf{g})$ are mutually orthonormal with respect to the probability measure of $\mathbf{Z}$. Therefore, the set $\{\Psi_i(\mathbf{z};\mathbf{g}), 1 \leq i \leq L_{N,m}\}$, constructed from the elements of $\mathbf{\Psi}_m(\mathbf{z};\mathbf{g})$, is linearly independent. Moreover, the set has cardinality $L_{N,m}$, which matches the dimension of the polynomial space of degree at most m [33]. As $m \to \infty$, $L_{N,m} \to \infty$ as well. In this case, the resulting set $\{\Psi_i(\mathbf{z};\mathbf{g}), 1 \leq i < \infty\}$ comprises an infinite number of basis functions. If the PDF of random input $\mathbf{Z}$ is compactly supported or is exponentially integrable [32], as assumed here, then the set of random orthonormal polynomials $\{\Psi_i(\mathbf{Z};\mathbf{g}), 1 \leq i < \infty\}$ forms an orthonormal basis

of $L^2(\Omega_{\mathbf{d}}, \mathcal{F}_{\mathbf{d}}, \mathbb{P}_{\mathbf{d}})$. Consequently, any output random variable $h(\mathbf{Z}; \mathbf{r}) \in L^2(\Omega_{\mathbf{d}}, \mathcal{F}_{\mathbf{d}}, \mathbb{P}_{\mathbf{d}})$ can be expanded as a Fourier series comprising multivariate orthonormal polynomials in $\mathbf{Z}$, referred to as the GPCE of [‡]

$$h(\mathbf{Z}; \mathbf{r}) \sim \sum_{i=1}^{\infty} C_i(\mathbf{r}) \Psi_i(\mathbf{Z}; \mathbf{g}), \tag{A.9}$$

where the expansion coefficients $C_i \in \mathbb{R}$, $i = 1, \ldots, \infty$, are defined as

$$\begin{aligned} C_i(\mathbf{r}) &:= \mathbb{E}_{\mathbf{g}}[h(\mathbf{Z}; \mathbf{r}) \Psi_i(\mathbf{Z}; \mathbf{g})] \\ &:= \int_{\bar{\mathbb{A}}^N} h(\mathbf{z}; \mathbf{r}) \Psi_i(\mathbf{z}; \mathbf{g}) f_{\mathbf{Z}}(\mathbf{z}; \mathbf{g}) d\mathbf{z}. \end{aligned} \tag{A.10}$$

According to [33], the GPCE of $h(\mathbf{Z}; \mathbf{r}) \in L^2(\Omega_{\mathbf{d}}, \mathcal{F}_{\mathbf{d}}, \mathbb{P}_{\mathbf{d}})$ converges in mean-square, in probability, and in distribution.

The GPCE contains an infinite number of orthonormal polynomials or coefficients. In a practical setting, the number must be finite, meaning that the GPCE must be truncated. However, there are multiple ways to perform a truncation, such as those involving tensor-product, total-degree, and hyperbolic-cross index sets. In this work, the truncation stemming from the total-degree index set is considered, as done in the previous work [33], which entails retaining polynomial expansion orders less than or equal to $m \in \mathbb{N}_0$. The result is an mth-order GPCE approximation

$$h_m(\mathbf{Z}; \mathbf{r}) = \sum_{i=1}^{L_{N,m}} C_i(\mathbf{r}) \Psi_i(\mathbf{Z}; \mathbf{g}) \tag{A.11}$$

of $h(\mathbf{Z}; \mathbf{r})$, comprising $L_{N,m}$ basis functions or expansion coefficients defined by Eq. (A.10). According to Eq. (A.1), the GPCE approximation in Eq. (A.11) is truncated according to a total-degree index set $\mathcal{J}_m$.

Note that the GPCE in Eqs. (A.9) and (A.11) should not be conflated with that of [57]. The GPCE, presented here, is meant for an arbitrary dependent probability distribution of random input. In contrast, the existing PCE, whether classical [58] or generalized [57], still needs independence of random input.

APPENDIX B. CALCULATION OF EXPANSION COEFFICIENTS

The definition of expansion coefficients $C_i(\mathbf{r})$, $i = 1, \ldots, L_{N,S,m}$, of an S-variate, mth-order DD-GPCE approximation $h_{S,m}(\mathbf{Z}; \mathbf{r})$ mandates various high-dimensional integrations. For an arbitrary function h and an arbitrary probability distribution of random input $\mathbf{Z}$, their exact evaluations from the definition alone are impractical. Numerical integration entailing a multivariate, tensor-product Gauss-type quadrature rule is computationally intensive, if not prohibitive, for high-dimensional ($N \geq 10$, say) RDO and RBDO problems. To resolve this difficulty, standard least-squares (SLS) was employed to estimate the coefficients. Here, only a brief summary of SLS is given for the paper to be self-contained. For additional details, readers are advised to consult a related work [33].

From the known distribution of random input $\mathbf{Z}$ and an output function $h : \bar{\mathbb{A}}^N \to \mathbb{R}$, consider an input-output data set $\{\mathbf{z}^{(l)}, h(\mathbf{z}^{(l)}; \mathbf{r})\}_{l=1}^{L}$ of size $L \in \mathbb{N}$, where $\mathbf{r}$ is decided from the knowledge of $\mathbf{d}$ and $\mathbf{g}$, as discussed earlier. The data set, often referred to as the experimental design, is generated by calculating the function h at each input data $\mathbf{z}^{(l)}$. Various sampling methods, namely, standard MCS, quasi-MCS (QMCS), and Latin hypercube sampling, can be used to build the experimental design. Using the experimental design, the approximate DD-GPCE coefficients $\tilde{C}_i(\mathbf{r})$, $i = 1, \ldots, L_{N,S,m}$, satisfy the linear system

$$\mathbf{A}\mathbf{c} = \mathbf{b}, \tag{B.1}$$

where

[‡]Here, the symbol $\sim$ represents equality in a weaker sense, such as equality in mean-square, but not necessarily pointwise, nor almost everywhere.

$$\begin{aligned}\mathbf{A} &:= \begin{bmatrix} \tilde{\Psi}_1(\mathbf{z}^{(1)};\mathbf{g}) & \dots & \tilde{\Psi}_{L_{N,S,m}}(\mathbf{z}^{(1)};\mathbf{g}) \\ \vdots & \ddots & \vdots \\ \tilde{\Psi}_1(\mathbf{z}^{(L)};\mathbf{g}) & \dots & \tilde{\Psi}_{L_{N,S,m}}(\mathbf{z}^{(L)};\mathbf{g}) \end{bmatrix}, \\ \mathbf{b} &:= (h(\mathbf{z}^{(1)};\mathbf{r}), \dots, h(\mathbf{z}^{(L)};\mathbf{r}))^\intercal, \text{ and} \\ \mathbf{c} &:= (\tilde{C}_1(\mathbf{r}), \dots, \tilde{C}_{L_{N,S,m}}(\mathbf{r}))^\intercal. \end{aligned} \tag{B.2}$$

From Eq. (B.2), $\tilde{\Psi}_i(\mathbf{z}^{(l)};\mathbf{g})$ represents an estimate of $\Psi_i(\mathbf{z}^{(l)};\mathbf{r})$ due to approximations resulting from the construction of the monomial moment matrix in Section 3.2. According to SLS, the best set of expansion coefficients is estimated by minimizing the mean-squared residual

$$\hat{e}_{S,m} := \frac{1}{L}\sum_{l=1}^{L}\left[h(\mathbf{z}^{(l)};\mathbf{r}) - \sum_{i=1}^{L_{N,S,m}} \tilde{C}_i\tilde{\Psi}_i(\mathbf{z}^{(l)};\mathbf{g})\right]^2. \tag{B.3}$$

As a result, the SLS solution $\hat{C}_i,\ i = 1, \dots, L_{N,S,m}$, is obtained from

$$\mathbf{A}^\intercal\mathbf{A}\hat{\mathbf{c}} = \mathbf{A}^\intercal\mathbf{b}, \tag{B.4}$$

where $\hat{\mathbf{c}} := (\hat{C}_1(\mathbf{r}), \dots, \hat{C}_{L_{N,S,m}}(\mathbf{r}))^\intercal$ and the $L_{N,S,m} \times L_{N,S,m}$ matrix $\mathbf{A}^\intercal\mathbf{A}$ is referred to as the information or data matrix. Finally, the inversion of the data matrix, if it is positive-definite, produces the best estimate,

$$\hat{\mathbf{c}} = (\mathbf{A}^\intercal\mathbf{A})^{-1}\mathbf{A}^\intercal\mathbf{b} \tag{B.5}$$

of the approximate DD-GPCE coefficients. When using SLS, the number of experimental data must be larger than the number of coefficients, that is, $L > L_{N,S,m}$. Even if this condition is met, the experimental design must be carefully chosen to ensure that the resulting matrix $\mathbf{A}^\intercal\mathbf{A}$ is well-conditioned.